Suspended sediment behavior in a coastal dry-summer subtropical catchment: effects of hydrologic preconditions

A.B. Gray[a,*], J.A. Warrick[b], G.B. Pasternack[a], E.B. Watson[a,1], and M.A. Goñi[c]

[a]University of California, Davis, One Shields Avenue, Davis, CA 95616, USA

[b]United States Geological Survey, 400 Natural Bridges Drive, Santa Cruz, CA 95060, USA

[c]Oregon State University, 104 CEOAS Administration Bldg., Corvallis, OR 97331-5503, USA

* Corresponding author – Tel.: +1 530-752-1130; E-mail: abgray@ucdavis.edu.

[1]Current affiliation: United States Environmental Protection Agency, Atlantic Ecology Division, Narragansett, RI 02882, USA

Abstract

Variation in fluvial suspended sediment–discharge behavior is generally thought to be the product of changes in processes governing the delivery of sediment and water to the channel. The objective of this study was to infer sediment supply dynamics from the response of suspended sediment behavior to antecedent hydrologic factors. The Salinas River (California) is seasonally active, moderately sized, and potentially susceptible to lasting impacts of hydrologic event history because of aridity, high discharge variability, and in-channel terminating flows. Forty-five years of suspended sediment data from the lower Salinas and 80 years of hydrologic data were used to construct hydrologic descriptors of basin preconditioning and test the effects of these preconditions on suspended sediment behavior. Hydrologic precondition factors — including change in mean daily discharge and increasing elapsed time since the last moderate discharge event (~ 10–20 times mean discharge (Q_{mean})) — were found to have significant positive effects on discharge-corrected, fine suspended-sediment concentrations. Conversely, increased elapsed time since the last low discharge event (~ 0.1–0.4 times Q_{mean}), and the sum of low flow conditions over interannual time scales were found to cause significant negative trends in fine suspended sediment concentration residuals. Suspended sand concentrations are suppressed by increased elapsed time after threshold discharges of ~ 0.1–2 and 5–100 times Q_{mean}, and increased low to no flow days over time scales from 1 to 2000 days. Current and previous year water yield and precipitation magnitudes correlate positively with sand concentration. Addition of fine sediment from lower Salinas hillslope or channel sources

on the rising limb of the hydrograph is the major mechanism behind an overall positive hysteretic pattern, which was forensically supported by the annual occurrence of in-channel suspended sediment deposition by early season, channel terminating flows and by the flushing function of moderate hydrologic events found in this study. The importance of hillslope and/or channel fine sediment contributions proximal to the lower Salinas are further highlighted by the lack of control exerted by upper subbasin water provenance on fine suspended sediment concentration, while sand behavior is differentiated by upper basin water provenance. Investigation of suspension of bed-sized sediment showed that the channel bed could exert significant effects on fine and sand-sized suspended sediment dynamics, but this mediation for fine sediment was most likely small in terms of decadal-scale sediment budgets. The magnitude of the effects of hydrologic variables on sediment dynamics remains uncertain, but the factors identified here may play a significant role in water quality, if not long-term sediment flux to the ocean.

Keywords: suspended sediment transport; rating curves; antecedent conditions; small mountainous rivers; arid rivers

1. Introduction

Rivers of small to moderate size (~ 10^1–10^4 km^2) draining active margins are recognized as transporting the majority of terrestrial sediment to the oceans (Milliman and Syvitski, 1992). Sediment yields from their basins are often highly episodic, caused by rare high discharge floods (Gonzalez-Hidalgo et al., 2010; Wheatcroft et al., 2010).

Small rivers in dry-summer subtropical regions, such as coastal California, are particularly prone to episodic hydrologic event control on sediment discharge, as most precipitation occurs during a short winter season that occasionally produces intense storm events (Inman and Jenkins, 1999; Farnsworth and Milliman, 2003; Warrick and Mertes, 2009).

Sediment dynamics in systems with high discharge variability are further impacted by the deposition and/or reorganization of sediment in the channel by flow recession and ephemeral flows that terminate in the channel (López-Tarazón et al., 2011) as well as sediment supply augmentation or suppression associated with large precipitation/hydrologic events and prolonged periods of no precipitation (Lana-Renault et al., 2007). Basin preconditioning — the sequence and temporal proximity of events that impact hillslope and channel sediment supply — and the long-term implications of these events as well as slower, extensive alteration of the land surface and vegetation also play significant roles in altering fluvial sediment production, particularly in episodic systems (Lenzi and Marchi, 2000; Pasternack et al., 2001; Chakrapani, 2005; Gao and Josefson, 2012; Warrick et al., 2013).

Sediment transported in suspension accounts for the majority of particulate matter conveyed by rivers (Meade et al., 1990). Because of the difficulty in collecting suspended sediment data, suspended sediment transport for most rivers has been estimated through rating curves that relate suspended sediment concentration (C_{SS}) to water discharge (Q), as the latter is more easily measured and often available in longer time series (Horowitz, 2003). Early investigations into antecedent hydrologic effects on suspended sediment flux were primarily focused either on the association of regional

scale patterns in suspended load resulting from long-term precipitation and discharge characteristics (i.e., Langbein and Schumm, 1958) or watershed scale studies of the 'lag effect' during individual hydrologic events, which results from slower moving sediment pulses relative to the transmission of peak water discharge at the event scale (Heidel, 1956; Carson et al., 1973; Shi et al., 1985). Identification of the principal factors affecting suspended sediment behavior has been an active field of study since suspended sediment–discharge rating relationships were found to lack predictive power in smaller catchments (Walling, 1977; Syvitski et al., 2000; Warrick and Rubin, 2007; Sadeghi et al., 2008).

As the amount of suspended sediment moved by a river is generally limited by sediment supply rather than the transport capacity of channelized flow, the residual variability of C_{SS} beyond that explained by Q in a given watershed is usually the result of factors that affect erosional processes, the delivery of eroded sediment to the channel, or the trapping efficiency of the channelized system (de Vente et al., 2007). Sediment and water supply to the channel are controlled by the same major factors, namely precipitation distribution and intensity, basin structure (relief, substrate composition), and basin preconditions (moisture levels, vegetation states, disturbance states) (Wischmeier and Smith, 1978; Syvitski et al., 2000; Lana-Renault et al., 2007; Mano et al., 2009). Increased shear stress during floods can erode channel margins, scour away stabilizing structures such as vegetation, and activate landslide snouts adjacent to the channel in upper basin areas, all of which can lead to increased channel bank and hillslope sediment delivery (Kelsey, 1980; Benda and Dunne, 1997; Poesen and Hooke, 1997; Korup, 2012). Conversely, large events can flush the channel system of fine

sediment stores deposited by recessional or ephemeral flows and can exhaust intermediate storage of hillslope sediment supplies, which can lead to depressed sediment yields from subsequent discharges (Droppo and Stone, 1994; Walling et al., 1998; Brasington and Richards, 2000; Hudson, 2003; Constantine et al., 2005; Batalla and Vericat, 2009). Thus, the $C_{SS} \sim Q$ rating curve is an exercise in the use of discharge as a proxy for the master variables controlling sediment delivery to the stream of channelized flow, even though it will not capture the dynamics of these landscape and channel processes.

The overall goal of this study was to test the hypothesis that antecedent hydrologic conditions significantly control suspended sediment behavior. The specific objectives were to (i) develop variables representing basin preconditions from hydrologic and precipitation time series data and (ii) determine if variability in suspended sediment behavior could be explained using the precondition variables. As the Salinas River flows only intermittently during the year, it was posited that in-channel deposition of sediment from incipient flows, and the eventual reworking of this sediment, would have a significant effect on suspended sediment dynamics. The results of hydrologic precondition analysis were explored to infer the sediment supply processes at play. The most significant aspect of this work is that it provides an approach for incorporating event to interannual scale hydrologic precondition characterization into the process of deciphering sediment supply dynamics at the basin scale.

2. Study region characteristics

The ~ 11,000-km^2 Salinas River watershed drains a portion of the Central Coast

Ranges of California, USA, flowing from the SE to NW along the Rinconada fault zone between the Sierra de Salinas and Santa Lucia Mountains to the SW and the Diablo and Gabilan Ranges to the NE (Rosenberg and Joseph, 2009) (Fig. 1). Maximum relief is ~ 1900 m; average watershed bounding ridge heights are 750 m to the NE and 1200 m in the SW, with ridge crest height generally decreasing toward the mouth of the Salinas (Neagley et al., 1990). Mountainous highlands are mostly composed of Mesozoic-aged sedimentary and metasedimentary rock with some igneous intrusions, while the northern extent of the mainstem valley floor is Tertiary and younger alluvial fill (Nutter, 1901). Land cover in the Salinas watershed largely follows local relief, with steep forested terrain giving way downslope to chaparral/scrub in the wetter western hills and grassland in the drier eastern hills (Farnsworth and Milliman, 2003). Valley bottoms were mostly converted to irrigated agriculture with a small proportion of urbanization (Thompson and Reynolds, 2002).

Climate along California's central coast is dry-summer subtropical with most precipitation delivered by a few winter storms. The largest storms are produced during strong El Niño years (Farnsworth and Milliman, 2003; Andrews et al., 2004). Convection of western tropical moisture through westerly storm tracks generally leads to S–SW impingement of storms (Andrews et al., 2004). Because of the SE to NW orientation of the basin and its small size, such storms can simultaneously deliver precipitation to the entire watershed to produce the largest floods on record. Orographically forced precipitation in the SW mountain ranges coupled with the preponderance of smaller storms and prevailing storm tracks leads to average annual precipitation rates that are much higher (~ 1000 mm/y) than in the NE region (~ 300 mm/y) (Farnsworth and

Milliman, 2003).

Average annual suspended sediment load was previously calculated as 1.7–3.3 Mt using monthly and daily *Q* with log-linear rating curves (Inman and Jenkins, 1999; Farsworth and Milliman, 2003). Ongoing work in this system by the authors has found that suspended sediment load estimated from daily discharge data using a combination of sand and fine suspended sediment rating curves for temporal domains of distinct suspended sediment behavior resulted in an average annual load of ~ 2.2 Mt.

The Salinas is a losing stream with naturally transient flow and no surface water passing through the lower reaches for much of the summer. The aquifers in the alluvial valley are overdrafted for agriculture, causing saltwater intrusion. Three major dams emplaced from 1941 to 1965 on the San Antonio and Nacimiento tributaries, as well as the upper most reaches of the Salinas, moderate flow from a total of ~ 2100 km^2 of the Salinas watershed, primarily for groundwater recharge purposes (Fig. 1). Average sediment trapping efficiency for dams in the central California coastal region have been estimated as ~ 84% by Willis and Griggs (2003) with the simple Brune (1953) method. Estimations of trapping efficiency by the authors based on the methods of Brown (1943) and the improved Brune method from Heinemann (1981, 1984) place the Salinas basin reservoirs in the range of 94–99% for bulk sediment and ~ 90% or greater for fine sediment (clay and silt) trapping efficiency

United States Geological Survey (USGS) daily average *Q* gauging stations on the mainstem and on the Arroyo Seco tributary date to 1901 (A3, Arroyo Seco near Greenfield) and 1931 (S1, Salinas River near Spreckels), respectively (Table 1; Fig. 1). The confluence of the Arroyo Seco and the Salinas is located 1.36 and 1.74 river

kilometers below the nearest upstream gages on the Salinas (S3, Salinas River near Soledad) and the Arroyo Seco (A1, Arroyo Seco below Reliz Creek near Soledad), respectively. Below the Arroyo Seco/Salinas confluence is referred to as the 'lower Salinas' in this study, which bears two mainstem gages 28.41 km (S2, Salinas River near Chualar) and 51.92 km (S1, Salinas River near Spreckels) downstream, respectively, both of which have a mean discharge of ~ 10 m^3/s with a 2-year return flood of 100–200 m^3/s. The 100-year flood is estimated to be ~ 3000 m^3/s, as per log-Pearson Type III flood frequency analysis (USGS NWIS). The mouth of the Salinas River is 21.14 km downstream from S1 and remains closed to the Monterey Bay via impounding sand bars, except under conditions of high river discharge and/or strong ocean waves (Watson et al., 2013).

The Arroyo Seco is the only undammed tributary of the Salinas River originating from the wet, mountainous western side of the basin and is also the last major tributary to enter the Salinas. In contrast, the Salinas watershed upstream of the confluence with the Arroyo Seco (referred to hereafter as the 'upper Salinas') is generally low gradient and bordered by intensively irrigated agriculture, while the Arroyo Seco is the least developed subbasin in the Salinas system, with ~ 95% chaparral/blue oak forest land cover and steep terrain. Most of the Salinas channel is broad and sand-bedded, with complex, braided, base-flow inset channels and low sandy banks with highly variable vegetation coverage. Transition to a primarily gravel bed occurs high in the upper Salinas, below the mainstem dam, while the Arroyo Seco transitions to a sand bed just before its confluence with the Salinas. Sediment export from the Arroyo Seco has been shown to be dominated by the convergence of wildfire and subsequent large

precipitation events (Warrick et al., 2012). The flashy nature of discharge in the Arroyo Seco leads to large flows produced rapidly relative to the upper Salinas, which can lead to lower Salinas discharge events that are primarily expressions of Arroyo Seco runoff.

3. Data

3.1. Experimental design

This study attempted to determine the effect of antecedent hydrologic conditions on C_{SS} behavior and infer the physical mechanisms behind these effects, with a particular emphasis on the possibility of in-channel mediation. The first phase of this study involved testing the residuals of C_{SS}-Q behavior for correlations with variables describing antecedent hydrology and comparing C_{SS}-Q behavior between subgroups defined by hydrologic conditions. Physical mechanisms behind these behaviors were approached by investigating hysteresis, the effects of subbasin water provenance, and analysis of the evolution of suspended sediment particle size distribution in terms of discharge and long profile position.

3.2. Hydrologic data

This study was based on suspended sediment samples collected by the authors and historical USGS samples. Samples were collected for this study between water years 2008 and 2011 from bridges crossing the Salinas River at Davis Street (3.99 km river distance below S1) and the USGS gauging stations S1 and S2 (Figs. 1 and 2B; Table 1). Water years for this region begin October 1 of the previous calendar year and end on September 30 of the calendar year. Samples were collected as per Warrick et

al. (2012), except for the following modifications. In all cases, samples were retrieved from the water surface at cross-channel stations of ~ one-quarter, one-half, and three-quarters wetted channel width. Two 1-L samples from each cross-channel station were collected for (i) total suspended sediment concentration (C_{SS}) and (ii) particle size distribution analysis. One event was sampled at high resolution — 250-ml samples every 2–3 hours. All samples were measured volumetrically and then filtered through preweighed, combusted, Whatman GF/A, 0.7 μm glass fiber filters. Filters were dried at 60°C for > 24 h, cooled to room temperature under vacuum in a desiccator, and then weighted to ± 0.0001 g. Sample sediment mass was obtained by subtracting filter mass from total mass. The C_{SS} was then calculated by dividing sample sediment mass by water sample total volume.

Particle size distribution analysis began with centrifuging water samples at 3250 g in 500-mL bottles for 10 min. After removing the supernatant, the remaining sediment was transferred to 150-mL beakers and treated with unheated and heated 30% H_2O_2 aliquots to remove organic materials, dispersed with sodium metaphosphate solution, and run through a Beckman-Coulter LS 230 (Beckman Coulter Inc., Fullerton, CA, USA) laser diffraction granulometer using polarization intensity differential scattering (PIDS) as per Gray et al. (2010).

Suspended sediment samples were collected from the surface of the river, and for this reason coarse suspended sediment particles were expected to be underrepresented. Simple sediment suspension calculations by particle size based on the characteristics of the highest and lowest flows showed that fine particles in the silt to clay range (diameter (D) < 62.5 μm) should be uniformly distributed throughout the

vertical profile (Rouse, 1937, 1938; Hill et al., 1988). Thus, particle size distribution analysis was restricted to fine particles of $D < 62.5$ μm. For all samples containing coarse ($D > 62.5$ μm) sediments, values for fine suspended sediment concentration (C_{SSf}) were calculated by multiplying C_{SS} by the proportion of sediment occurring in the fine fraction:

$$C_{SSf} = \frac{C_{SS} \text{ x } (\% \text{ particles} < 62.5 \text{ μm})}{100} \quad (1)$$

The USGS collected flow-integrated C_{SS} samples from the Salinas River at locations corresponding to S1 and S2 from water years 1969 to 1986 and 1967 to 2010, respectively (USGS NWIS, 2013) (Fig. 2A). Bed sediment samples were also collected between 1967 and 1992. The particle size distribution of bed sediments at S1 and S2 was characterized by sieving on nine and six occasions, respectively, between 1967 and 1992.

The USGS suspended sediment data had to uniquely represent a given discharge event and be associated with both instantaneous Q and particle size data for inclusion in this study. Multiple samples collected during the same event at constant discharge were combined into single samples through simple averaging of C_{SS}, Q, and particle size distribution data. Most USGS suspended sediment samples were processed for particle size distribution by sieving to establish the relative contribution of coarse and fine fractions. The C_{SSf} for these samples was calculated using Eq. (1), and the concentration of sand-sized suspended sediment (C_{SSs}) was obtained by subtracting C_{SSf} from C_{SS}. Hereafter, the term C_{SS} is used as a general term for suspended

sediment concentration when referring to tests that were conducted separately on C_{SSf} and on C_{SSs}.

All suspended sediment data from the USGS were obtained with associated instantaneous discharge values. New samples collected in this study were assigned discharge values through linear interpolation between the two temporally nearest 15-min discharge data from the appropriate USGS gage. Discharge for Davis Street samples were obtained from the S1 record of 15-min discharge data, by lagging the time by the estimated transit time (t_t), where t_t was equal to the distance between Davis Street and S1 divided by the transit speed (m/s) of peak flow between S2 and S1 for each discharge event in question. Although transit speeds were found to be highly variable, ranging from 0.01 to 2.38 m/s, most values fell between 0.2 and 0.8 m/s. When the resultant lagged time fell between 15-min discharge records, the associated discharge was calculated through linear interpolation.

Field measurements of flow characteristics collected between 1974 and 2012 were used in hydraulic geometry calculations for sites S1, S2, S3, and A1, which were measured for instantaneous discharge, flow area (a), flow width (w), and average velocity (u) by the USGS between 1974 and 2012.

3.3. Precipitation data

Three National Weather Service monthly precipitation records were used in this study, including those from stations at Big Sur State Park (BGS), Priest Valley (PSV), and Salinas no.2 (SAP) (Fig. 1). The BGS gage is located outside of the Salinas watershed, just inland from the coast at 36.247° N., 121.811° W.; while PSV sits in the

central, western portion of the upper Salinas at 36.183° N., 120.700° W.; and SAP in the lower Salinas at 36.667° N., 121.667° W. The BGS data set contained the fewest gaps. Regression between log-transformed annual precipitation (*P*) and log-transformed annual water yield at S1 fitted by station also showed that more variation in water yield was explained by BGS than the other two precipitation stations, so BGS was used in further analyses. Precipitation data gaps for years 1981, 1982, and 1983 were reconstructed using the inverse of the water yield ~ precipitation rating curve.

3.4. Bias analysis

The effects of the inclusion of two sampling sites and the selection of certain samples for particle size distribution analysis by the USGS were found to not bias the ensuing analyses. For further details see Appendix A.

4. Suspended sediment rating curves and residuals

Available C_{SS} and associated Q data were used to model the dependence of C_{SS} on Q for the system (hereafter referred to in the form of C_{SS} ~ Q). A log-linear sediment rating curve describes this relationship through a linear regression fitted to log-transformed data in the form

$$log(C_{SS}) = log(a) + b\, log(Q) + \varepsilon \quad (2)$$

Log-linear rating curves were constructed for the entire lower Salinas C_{SSf} and C_{SSs} data set (USGS and data collected for this study at sites S1 and S2; Figs. 3A,B). These

rating curves accounted for a moderate proportion of variation in C_{SSf}, with r^2 values of 0.55 and a standard error of 0.63 log (mg/l) for the linear regression model and an r^2 value of 0.70 with a standard error of 0.60 log (mg/L) for C_{SSs}.

Rating curve residuals, which are the difference between sample values of C_{SS} and the value of the rating curve, can be used to reveal systematic departures in sample C_{SS} behavior from that of the rating curve model (Figs. 3C,D). Residual values plotted by discharge for lower Salinas fine suspended sediment show that the log-linear rating curve generally underestimated the lowest ($q < 1$ m^3/s) and highest ($q > 800$ m^3/s) discharge range C_{SSf} (positive rating curve residuals), and slightly overestimated moderate discharge range C_{SSf} (negative rating curve residuals) (Fig. 3C). The concentration of sand in suspension was also consistently underestimated for the lowest discharge range of $q < 1$ m^3/s (Fig. 3D). It has been recognized that the $C_{SS} \sim Q$ relationships of many episodic river systems on the west coast of North America often systematically depart from the log-linear rating curve, particularly at low and high discharge (Farnsworth and Warrick, 2007; Warrick et al., 2013).

To avoid potential bias from the systematically poor fit of log-linear curves, LOESS curves were fitted to the $C_{SS} \sim Q$ data sets for subsequent residual analysis, as well as particle size distribution estimation, using $\alpha = 0.75$ and second-degree polynomials (Cleveland, 1979; Cleveland and Devlin, 1988; Helsel and Hirsch, 2002). LOESS curves fit to each of the entire fine and sand data sets produced standard errors of 0.59 and 0.55 log(mg/L), respectively (Figs. 3A,B). LOESS residuals for fine sediment appeared to have low structure with discharge (Figs. 3E,F). This was confirmed by sequential summation of linear regression and LOESS residuals over the discharge

domain, as LOESS rating curves displayed less persistent dependence on discharge than the corresponding linear regression curves (Figs. 3G,H). Note that rating curves in this study were not adjusted for log-transform bias (i.e., Ferguson, 1986), as they were used solely for intercurve comparison rather than prediction of C_{SS} in terms of untransformed units of measure.

5. Antecedent hydrologic conditions

5.1. Hydrologic variable effects on C_{SS}-Q residuals

Hydrologic variables representing event conditions, basin wetness, seasonality, basin aridity, and hydrologic event history were computed from discharge data to account for variability in suspended sediment concentration not explained by instantaneous discharge (Table 2). Event scale hydrology was described using the change in daily discharge (ΔQ_d), calculated as

$$\Delta Q_d = Q_{dts} - Q_{dts-1} \quad (3)$$

where Q_{dts} is the mean daily discharge value for the day of a given C_{SS} sample, and Q_{dts-1} is the mean daily discharge value for the day before the sample. Basin wetness was represented by lower Salinas annual water yield computed from mean daily discharge at S1 and annual precipitation at BGS for the current and previous water years. The effects of seasonality and basin aridity were both examined through the set of variables called $\Sigma Q_{0.1}$, calculated as the sum of days that satisfied the hydrologic argument of daily average $Q \leq 0.1$ m^3/s in a given t_{s-1} to t_{s-x} temporal window, where t_s is

the day that a given C_{SS} sample was collected and x is the number of days prescribed by the sampling window. The value of 0.1 m^3/s was chosen because of the accuracy of the hydrologic gages in the lower Salinas, whereby flows ≤ 0.1 m^3/s could be considered as 'no-flow' conditions. The $\Sigma Q_{0.1}$ variable set was generated by calculating $\Sigma Q_{0.1}$ for each suspended sediment sample using sampling windows from 1 to 2000 days, in one-day increments. Shorter sampling windows (~ 10–100 days) tested season-scale effects, as lower Salinas discharge during the summer dry season is often < 0.1 m^3/s. Longer sampling windows (200–2000 days) tested the effects of extended low/no flow conditions as well as aridity. Hydrologic event history was represented by the variable Q_j *time*, which is a measure of the elapsed time between the last daily average Q value ≥ a given threshold discharge magnitude (Q_j) and the date of collection for each C_{SS} sample. The set of Q_j *time* variables were created by varying Q_j from 1 to 1000 m^3/s in 1-m^3/s steps.

The effect of hydrologic variables on (C_{SS} ~ Q) LOESS residuals was tested with the nonparametric Mann-Kendall trend analysis using the R package 'Kendall' (McLeod, 2011; R Development Core Team, 2012). Mann-Kendall T values indicate the strength and direction of monotonic trends, with -1 and 1 representing perfectly negative and positive monotonic trends, respectively, along with p-values used to assess significance (Helsel and Hirsch, 2002).

5.2. Hydrologic variable test results

Fine and sand-sized sediment responded differently to antecedent hydrologic conditions. Fine sediment concentration was found to a have a weak though significant,

positive correlation with ΔQ_d (Table 3). The set of variables $\Sigma Q_{0.1}$ produced consistently negative and significant trends for summation windows between ~ 1150 and 2000 days, with slightly stronger (larger T magnitude) correlations found with increasing summation window size (Fig. 4A). This suggests that long-term arid conditions decreased fine sediment supply. The set of hydrologic event history variables (Q_j *time*) produced significant negative trends in fine suspended sediment rating curve residuals with increasing elapsed time since the last low flow ($Q \geq 1$, 2, and 4 m^3/s), while moderate events of ~ 100 to 200 m^3/s produced significant positive trends in residuals with increasing elapsed time (Fig. 5A). The former result is evidence that sediment supply is suppressed by prolonged low flow (dry) conditions, while the latter provides some insight into how wetter conditions, resulting in moderately high discharges, may act as flushing functions, decreasing fine sediment supply for a time after the event.

Sand concentration exhibited significant positive correlations with wet conditions, and negative correlations with dry conditions (Table 3). Significant negative trends were found for sand-sized suspended sediment residuals and the entire $\Sigma Q_{0.1}$ variable set, from window sizes 1–2000 d (Fig. 4B). Significant negative trends were found in (C_{SSs} ~ Q) residuals for the Q_j *time* variable set for Q_j values between 1–20 and 50–1000 m^3/s, which also points to a general decrease in sand-sized sediment supply with less discharge in the lower Salinas (Fig. 5B). Larger T magnitudes— indicating stronger monotonic trends — were found at $Q_j \approx 400$ m^3/s and $\Sigma Q_{0.1}$ for summations windows of ~ 75–100 days, suggesting perhaps threshold sediment supply production associated with discharges around 400 m^3/s and a seasonal suppression of sand supply for flows after the summer dry season.

Although Mann-Kendall tests are not as sensitive as linear regression to outliers positioned at the beginning or end of data series, problems with outliers can arise. Furthermore, proper use of the Mann-Kendall test requires that the dependent variable response is monotonic in relation to the independent variable. Values of C_{SS} ~ Q LOESS rating curve residuals were plotted against $\Sigma Q_{0.1}$ and Q_j *time* values found to be significant (Fig. 6). All linear regressions, added for illustrative purposes, were found to be significant, except for fine suspended sediment residuals vs. $\Sigma Q_{0.1}$ variables, which appeared to be compromised by nonlinear responses (Figs. 6A,B,C). The other representative scatter plots reveal generally monotonic structures that do not appear to be highly steered by outliers, with the exception of the response of fine sediment to the Q_j *time* variable at j = 200 m^3/s (Fig. 6F), which was highly steered by a few values above 1500 d (results not shown).

Analysis of hydrologic variables showed that the behaviors of fine and sand fractions in the lower Salinas River are affected by hydrologic event history. But which pools of sediment are impacted by these factors: the hillslope, channel banks, or channel bed? The remainder of this study is oriented toward this question.

6. Effects of hydrographic position and flow regime

6.1. Rating curve subgroup comparison with ANCOVA

The first step toward deciphering process was to test for differences in C_{SS} behavior resulting from hydrographic position and flow regime. The C_{SS} data sets were split into subgroups (rising/falling or storm/winter recessional/summer base flow, respectively). Log-linear rating curves were then fitted to each subgroup and tested for differences in

behavior. An ANCOVA approach was used to determine if the rating curves were statistically 'coincident' (indistinguishable), and if not, whether they differed in rating curve slope or offset. The homoscedasticity of all hydrologic position subsets was tested using a two sample *F*-test statistic (e.g., Larsen, 2003). In all cases the subgroups were found to be homoscedastic unless otherwise noted. For a detailed account of the ANCOVA approach to comparing rating curves, see Appendix A.

Flow regime assignment was determined by examination of the precipitation record at BGS and discharge at S1, S2, and S3. Samples were identified as originating from storm flow if they were collected during the rising or falling limb of a hydrographic event that occurred because of precipitation, with the end of the falling limb identified as a change in concavity. This was visually assessed for those samples that were located far from the concavity change or found by computing the second derivative of a fitted fourth-order polynomial when samples were proximal to the shift. Winter recessional samples were those that were collected during the precipitation season but after the end of a given falling limb. The precipitation season was determined by examination of the monthly precipitation record. Summer base flow samples were those collected after the final falling limb of the winter precipitation season.

6.2. Rating curve subgroup ANCOVA results

Hydrologic variable correlation analyses indicated significant differences in (C_{SSf} ~ Q) behavior with ΔQ_d, while previous studies suggested that there may be large differences in suspended sediment behavior between different flow regimes (i.e., storm, winter recessional, and summer base flow) for most rivers (e.g., Walling, 1977; Estrany

et al., 2009). A trend in C_{SSf} dependence on ΔQ_d implies that consistent hysteretic patterns in C_{SSf} behavior based on hydrographic position may occur in the system. Fine sediment from rising limb samples was found to have a greater slope than falling limb samples and a slightly higher offset (Fig. 7A), while the sand-sized hydrologic position rating curves were almost identical (Fig. 7B). Results of the ANCOVA tests indicated that the rating curves for the fine suspended sediment hydrologic position subgroups could be considered parallel and offset equivalent, but were not coincident; while the rising and falling limbs of sand-sized suspended sediment were statistically coincident (Table 4; Fig. 7 A,B). ANCOVA results for storm, winter recessional, and summer base flow rating curves were not significantly different in terms of parallelism, offset, or total coincidence, nor were the summer and winter recessional flow curves (Table 4; Fig. 7 C,D). Thus a weak hysteretic pattern was evident for fine suspended sediment, but not sand, over the entire sample record; while no evidence was found of flow regime control on suspended sediment concentration.

7. Suspended sediment hysteresis

7.1. Hysteresis identification

The next step in the investigation of physical processes was to examine event-scale patterns in suspended sediment hysteresis. Six events sampled by the USGS between 1970 and 1978 and two by the authors in 2010 were sampled sufficiently for some degree of fine sediment hysteresis determination. Sampling resolution from the USGS data set was also sufficient to compare fine and sand-sized sediment behavior over the course of seven events. 'Positive' hysteresis occurs when rising limb C_{SS}

values are larger than C_{SS} values of corresponding discharge magnitude on the falling limb, while 'negative' hysteresis occurs because of the opposite effect (Hudson, 2003). Log-log plots of sequential samples collected over a given discharge event, with C_{SS} on the ordinate and Q on the abscissa, were used to assess the presence of hysteresis.

7.2. Hysteresis results

Only eight hydrologic events were sampled sufficiently for some insight into event scale hysteretic behavior of fine sediment; of these, six were sampled at S1 and two at S2 (see Fig. 8). Log-log plots of C_{SSf} against Q revealed evidence for positive, negative, and mixed positive/negative hysteretic patterns for five events with low to moderate peak discharges (~ 10–100 m^3/s; see Figs. 8A-E) and evidence of positive hysteresis for three high peak discharge events (~ 250, 450, and 1600 m^3/s, respectively, which were the peak discharge events for water years 1974, 1973, and 1978, respectively, see Figs. 8G,H). Sample density for most of the events with indications of positive or negative behavior was not sufficient to rule out more complex, mixed hysteretic; behaviors, however, these plots do show that the lower Salinas fine suspended sediment exhibited positive and negative hysteresis behavior over a wide range of discharges.

Although few events were sampled sufficiently for determination of sand hysteresis, seven were sampled adequately for comparisons of rising/falling limb behavior between the fine and sand fractions of suspended sediment (Fig. 9). Three events showed fine and sand-sized sediment behaving very similarly, with indications of negative (Figs. 9A–D) and positive (Figs. 9E,F) hysteresis. For those events when the

rising/falling limb relationship of fine and sand fraction behavior was found to differ, it consistently manifested as an increase in the concentration magnitude of falling limb samples relative to rising limb samples in the sand fraction (Figs. 9G–N). Next, the potential mechanisms associated with hysteretic behavior in the lower Salinas were assessed by examining subbasin routing effects on C_{SS} behavior (section 8) and channel bed contributions to suspended sediment (section 9).

8. Effects of subbasin water provenance

8.1. Routing analysis

Hysteresis in C_{SS}-Q relationships in rivers of moderate to large size can result from differences in subbasin suspended sediment dynamics (Shi et al., 1985; Asselman, 1999). Examination of the potential for such routing effects on C_{SSf} in the lower Salinas was motivated by a bifurcation of the Salinas system that occurs 28.4 km upstream from S2, at the confluence of the Salinas and Arroyo Seco (Fig. 1; Table 1). Because of large differences in subbasin characteristics, differential contribution of the upper Salinas and the Arroyo Seco could be a major driver of hysteretic suspended sediment behavior.

Identification of lower Salinas sampled flows that were dominated by contributions of the upper Salinas or the Arroyo Seco and testing of these subgroups for differences in C_{SS}-Q behavior allowed for a joint assessment of the potential differences in subbasin suspended sediment behavior and the attenuation of this signal downstream. The entire lower Salinas fine and sand-sized suspended sediment data sets were sorted into those samples grossly dominated by one tributary or the other by

following peak flow transmission of daily discharge data from gages throughout the basin. Because of the low temporal resolution of the discharge data (daily average *Q*) that could be used for samples collected before 1989, only 198 of the 330 fine sediment and 123 out of 248 sand-sized sediment sampled discharges were identified as originating primarily from one of the two subbasins. The data set was then trimmed of upper Salinas data points from the lowest and highest discharges in order to match the discharge range of the Arroyo Seco dominated subset to remove the potential bias of rating curves calculated over different ranges of discharge. These 'dominant tributary' subsets were then tested using the ANCOVA methodology (see section 6.1 and Appendix A).

8.2. Routing results

No significant differences in C_{SSf}-*Q* behavior were identified between the Arroyo Seco and upper Salinas dominated flows (Table 4; Fig. 10A). Significant differences were found in terms of slope and offset for sand-sized suspended sediment rating curves partitioned by subbasin, with Arroyo Seco dominated samples resulting in a lower slope and higher offset (Table 4; Fig. 10B). Thus, subbasin water contribution control on fine suspended sediment behavior in the lower Salinas was eliminated as a significant contributing mechanism to the overall positive hysteresis observed in fine suspended sediment in the lower Salinas, implicating significant lower Salinas control on fine sediment dynamics, and more distributed control of sand-sized sediment.

9. The channel bed and suspended sediment

9.1. Channel bed analyses

In the absence of an intensive channel-oriented field campaign, here the possibility of significant lower Salinas channel mediation of suspended sediment behavior through storage and resuspension of suspended sediment material was addressed through comparative particle size distribution characteristics between the channel bed and suspended sediment pools at S1 and S2 and through estimation of fine sediment content of the channel bed. Hydraulic geometry relationships were also calculated to assess how the lower Salinas flow characteristics changed with discharge.

Average particle size distribution characteristics were compared for bed sediment at stations S1 and S2 and suspended sediment samples in relation to discharge. Log-linear rating curves were constructed for USGS suspended sediment samples by standard USGS particle size classes of whole ϕ intervals as well as the sand fraction that accounted for most of the bed sediment at both S1 and S2 (125 to 2000 μm) over the range of discharges shown to approximate log-linear behavior for C_{SSf} and C_{SSs} ($q \geq 1$ m^3/s). Particle size range rating curves were then compared by station (S1, S2) using the ANCOVA methods introduced in section 6. Suspended sediment concentration of particle size ranges that behaved in a statistically coincident manner between sites were then described by LOESS rating curves computed from joint S1 and S2 data, while size ranges with significantly different log-linear behavior were described with separate rating curves by station. Average particle size distributions by percent mass for each station for discharges spanning five orders of magnitude (0.1–1000 m^3/s) were calculated from the particle size range LOESS curves. Particle size distribution

characteristics and average lower Salinas channel width from S1 to S2 were used to estimate the mass of bed sediment by particle class for the top 10 cm of reach channel surface assuming a planimetric channel for simplicity of calculation. Width, average depth (*d*), and mean velocity were related to *Q* through a power law function with exponential terms of *b*, *f,* and *m,* respectively, for sites S1, S2, S3, and A1 (Leopold and Maddock, 1953).

9.2. Channel bed results

Rating curves constructed for each standard USGS particle size range by station exhibited very little difference in suspended sediment behavior between S1 and S2 for clay and silt particle sizes, although some sand classes appeared to increase in concentration between S1 and S2 (linear rating curve comparison not shown).This observation was confirmed by ANCOVA tests, which showed no statistically significant difference in rating curves between stations for all particle size ranges except 62.5–125, 125–250, and 125–2000 μm sands. In each of these sand ranges, the condition of coincident rating curves was significantly violated, mostly because of differences in rating curve offsets, which were just below the $p < 0.05$ threshold for significance (Table 4). Thus some sand concentrations slightly increase downstream from station S2 to S1, including the broad range encompassing most bed-sized sediment ($d > 125$ μm), but fine suspended sediment concentrations behave identically between stations.

Lower Salinas C_{SS} ~ Q LOESS rating curves by texture classes (clay, silt, and sand) showed that clay-sized particles rapidly become dominant between 0.1 and 1 m^3/s and remain so for all higher flows (Fig. 11A). Sand C_{SS} values increase rapidly between

1–10 m^3/s to join the silt curve, and the two follow nearly the same path for much of the discharge range between 10 and 1000 m^3/s. Particle size range LOESS curves (Figs. 11B–E) were used to compute average particle size distributions at S1 and S2 for discharge classes 0.1, 1, 10, 100, and 1000 m^3/s (Fig. 12). Differences in suspended sand behavior between S1 and S2 were evident in the evolution of sharp, single-peaked sand distributions at S1 with increasing discharge from 1 to 100 m^3/s, in comparison to the maintenance of a low percentage, flat-peaked sand distribution at S2 (Figs. 12C–H).

The average bed sediment composition between 1967 and 1992 at stations S1 and S2 was 2.7 and 5.2% fines ($d < 62.5$ μm), respectively (Figs. 12K,L). Assuming a bulk density of 1.3 g/cm^3 for fine sediment, the channel bed at these sites could potentially yield 0.35–0.68 g/cm^2 of fines in the top 10 cm. Applying the average of these values and assuming the average flow width measured by the USGS at S1 and S2 of 161 m, a gross estimate of available fine in the reach between S1 and S2, and between S2 and S3 is ~ $2 \cdot 10^4$ and $2.4 \cdot 10^4$ tons of fine sediment, respectively.

The results of hydraulic geometry analysis at S1, S2, S3, and A1 showed a dominance of width response to flow changes (Table 5). Depth was more responsive than velocity at Salinas sites, while the inverse was true for the steeper, rougher Arroyo Seco site; however, all four sites primarily responded through width adjustment. Because the capability to entrain sediment is dependent on stream power (in steady, uniform flow), which is dependent on depth, the ability to erode and transport sediment increases relatively slowly with discharge at these sites (Leopold and Maddock, 1953; Kale and Hire, 2004).

10. Discussion

10.1. Synthesis

The following antecedent hydrologic condition effects on suspended sediment behavior were found for the lower Salinas River:

- Fine sediment concentration decreased with:
    - Dry conditions over interannual time scales
    - Falling flows
- Fine sediment concentration increased with:
    - Rising flows
    - Longer elapsed time since the last moderate flow (10–20·Q_{mean})
- Sand concentration decreased with:
    - Dry conditions over seasonal to interannual time scales
    - Upper Salinas water provenance for 10–50·Q_{mean} flows
- Sand concentration increased with:
    - Wetter conditions during the current and previous water year
    - Recent flow activity
    - Upper Salinas water provenance for low flows (< Q_{mean})

Prolonged dry conditions were found to reduce both fine and sand-sized suspended sediment concentrations. No significant seasonal signal was observed for fine sediment in the lower Salinas, while sand supply to the suspended sediment transport appears to be strongly linked to preceding discharge magnitudes and to the amount of time that the channel experienced very low to no flow conditions over

temporal scales that range from days to years. Fine sediment concentrations also increased in the lower Salinas with increasing elapsed time since moderate discharges of around 100–200 m^3/s, long periods of which were also associated with prolonged droughts. Thus, there appear to be competing factors influencing fine sediment response to prolonged dry conditions, while sand supply is consistently suppressed.

The decrease in sand-sized sediment after the dry season and decreases in both fine and sand-sized sediment over seasonal to interannual periods of dry conditions is contrary to the pattern of sediment exhaustion commonly observed over the course of the wet season monsoonal systems (Paustian and Beschta, 1979; McCulloch et al., 2003; Kale and Hire, 2004; López-Tarazón et al., 2010; Warrick et al., 2013). The phenomenon of seasonal and interannual decreases in suspended sediment during dry periods in the lower Salinas may be caused in part by changes in surface erodiblility. In coastal dry-summer subtropical climates such as that of the Salinas with warm, dry summers and cool, wet winters, the lack of flow and elevated temperatures of the summer dry season may dry out surficial channel sediments, particularly since the lower Salinas River bed is perched above groundwater. Fine, cohesive sediment is generally more difficult to entrain with increased deposition age, as interparticle bonding strength can increase drastically with dewatering; subaerial exposure can also lead to increases in the hydrophobicity of sediment (Mehta et al., 1989; Winterwerp et al., 1990). Prolonged intervals of low to no-flow conditions could also reduce channel and hillslope sediment contribution through the incursion of vegetation in channels, gullies, and other intense precipitation/discharge-induced land surface disturbances such as slumps and mass wasting scars. Thus, summer dry seasons and multiyear droughts could lead to

fine sediment that is less likely to be entrained, and once entrained more difficult to convey given increased roughness in vegetated channels, particularly in the case of early season flows that often must wet the channel and encounter vegetation not yet disturbed by flow. These possibilities remain to be tested in the field.

The flushing function of moderate discharges found for fine sediment in the lower Salinas is an understudied phenomenon, perhaps because of the focus on decadal to centennial scale sediment yield within the research community. Much of the work on hydrometeorological event preconditioning has focused on the effect of large, infrequent floods that generally transport large proportions of interdecadal sediment budgets and have been shown to have lasting geomorphic and sediment supply effects in steep, mountainous rivers on active margins (Brown and Ritter, 1971; Kelsey, 1980; Madej and Oseki, 1996; Warrick et al., 2013), although there has been some interest in terms of dam-release functionality (e.g., Batalla and Vericat, 2009). Sand concentrations on the other hand seem to be stimulated by ever larger and more recent hydrologic events, which is consistent with the northern California coast range systems that have exhibited increases in sediment supply immediately following large precipitation/discharge events, such as the widespread flooding of the December 1964 event (Warrick et al., 2013). Thus, fine and sand-sized sediments in the lower Salinas respond differently to previous hydrologic events, with sand supplies enriched by more recent and larger flows and fine sediment decreased after moderate threshold events.

10.2. Event characteristics and routing

Why do fine sediment and sand respond differently to antecedent hydrologic

events? Fine suspended sediment sources in most rivers – including moderately sized, steep coastal basins such as the Salinas – are generally known to be dominated by hillslope wash load, while sand supplies are often moderated to some degree by lower mainstem channel storage and transport competency (Walling and Moorehead, 1987). However, the Salinas River channel must moderate fine sediment transport to some extent, as suspended load must deposit when flows terminate in the channel with complete loss to recharge. Investigation into event characteristics, hysteresis, water provenance, and evolution of particle size distribution with discharge magnitude and downstream position provided evidence that the Salinas channel does indeed influence both sand and fine suspended sediment behavior.

The positive correlation between ΔQ_d and fine suspended sediment concentration suggests that the conditions leading to rapid increases in discharge, namely increased wash load resulting from the erosivity of intense precipitation events, and/or the energy imparted to the channel by rapid increases in discharge are significant contributing factors to positive fine suspended sediment hysteresis in the lower Salinas. The ΔQ_d variable employed in this study is similar to the *Flashiness Index* (*FI*) developed by Batalla and Varicat (2009), where $FI = \Delta Q/t$, which has been successfully used as an index for energy expenditure on the channel (e.g., Tena et al., 2011). Fine suspended sediment in the lower Salinas displayed positive and negative hysteretic behavior with discharge, but the positive correlation with ΔQ_d indicated that positive hysteresis effects slightly dominated the record. The major mechanisms generally associated with positive hysteresis include hydrodynamic phenomena such as increased boundary shear stress/shear velocity on the rising limb of the hydrograph

because of a greater water surface slope than on the falling limb (Garcia and Parker, 1991), a larger proportional contribution of base flow/interflow on the falling limb (Gao and Pasternack, 2007), and routing considerations such as higher fine particle sediment supply from areas proximal to the channel and/or lower in the basin (Williams, 1989). Negative hysteresis has primarily been associated with routing characteristics, including higher sediment supply from distal portions of the basin and sediment transport lag in larger (> 10^3 km^2) basins, because suspended sediment downstream particle velocities are often lower than peak discharge wave celerity (Heidel, 1956; Williams, 1989). The provenance of storm waters above the lower Salinas was not a significant factor in determining C_{SSf} for low to moderate flows, which indicates that upper basin wash load signals attenuate before reaching the lower Salinas stations. This is counterintuitive, as the Arroyo Seco and the upper Salinas are on average very different subbasins in terms of relief, area, vegetation and soil characteristics, and fire regimes (Farnsworth and Milliman, 2003; Warrick et al., 2012); and one would expect wash load signatures to differ, as more moderate differences in subbasin characteristics have been shown to cause significant differences in suspended sediment behavior (e.g., Ankers et al., 2003).

10.3. Channel mediation

Thus upper basin provenance effects on fine sediment are overprinted by some combination of the following lower Salinas sediment sources: runoff, channel bed, and/or bank sediment. Routing analysis samples were identified by subbasin peak flow events and therefore, by definition, composed of very little lower Salinas storm water.

This issue coupled with the fact that suspended sediment is deposited in the Salinas mainstem channel by early and late season flows, the evidence that C_{SSf} values increase with increasing energy imparted to the channel, and the lack of effect of hydrologic mode (summer base, storm, or winter recessional flow) on low flow C_{SS} supports the notion that lower Salinas fine suspended sediment dynamics for flows up to ~ $50 \cdot Q_{mean}$ are significantly affected by in-channel processes such as bank erosion as well as deposition and resuspension of fine sediment. Furthermore, much of the flow range sampled for the paired subbasin dominance analysis was below bankfull for the lower Salinas, which generally has a wide, complex channel composed of bar forms in various states of vegetation and multiple low water channels, as evidenced by the fact that lower Salinas hydraulic geometry changes most rapidly in width with increasing discharge. Therefore channel bank sediment control is probably not the major mechanism at play, as the banks of the lower Salinas are not interacting with flow over much of this discharge range. Thus, the lower Salinas appears to significantly alter upper basin fine suspended sediment signals toward a uniform behavior based primarily on in-channel dynamics at low to moderate water discharges. However, differences in sand-sized sediment behavior did persist to the lower Salinas, which suggests that subbasin sand signals are stronger than the overprinting of lower Salinas in-channel processes.

Bed and suspended sediment particle sized distribution analyses showed that bed sands likely play an increasing role in lower Salinas suspended sediment with increasing discharge, which is unsurprising as coarser sands are often transport limited in sand-bedded rivers. Moderate flows (~ 100 m^3/s) found to cause a decrease in

subsequent fine sediment concentration were accompanied by the highest proportion of bed-sized sediment at station S2 and especially S1 (Fig. 12). Increases in channel bed mobility exposing intermixed fines and the resuspension of surficial channel-deposited fines that otherwise slowly re-enter the water column over time may play a role in flushing associated with events of these magnitudes. The flushing effect may also operate on the hillslope by exhausting surficial, easily mobilized sediment, as the hillslope sediment pool is far larger than that of the channel (Inman and Jenkins, 1999). Determination of the proportional role of channel and hillslope sediment sources is beyond the scope of this study, but further evidence does support the significance of in-channel processes.

The lower Salinas appears to be insensitive to flow regime differences over low to moderate discharge magnitudes (Table 4). Previous studies have shown that precipitation-driven storm flows often display dramatically different suspended sediment behavior in comparison to flows attributed to interflow, ground water discharge, or recharge-oriented dam releases (winter recessional or summer base flow), due primarily to the increased contribution of hillslope and channel margin sediment from precipitation events (Lana-Renault et al., 2007; López-Tarazón et al., 2010; Oeurng et al., 2010; Tena et al., 2011; Gao and Josefson, 2012). Lack of sensitivity in the lower Salinas further supports the idea that the channel plays a significant role in moderating suspended sediment concentration as water routed overland, through interflow or groundwater; and summer dam releases, which are almost devoid of sediment, are statistically coincident in suspended sediment rating curve behavior at low to moderate flow magnitudes. Previous studies have found that fine sediment may penetrate deeply

into the coarser channel matrix and that these fines re-enter suspension only by flows large enough to mobilize bed sediment, even in reaches where bed sediment was sandy (López-Tarazón et al., 2011). Therefore, if the channel bed is generally of low mobility, surficial and intermixed channel deposits of incipient and recessionary flows may contribute significantly to the fine sediment load of low flows.

In-channel storage has been found to play a significant role in fine sediment dynamics in other rivers, with fine sediment content of 0.04–8.0 g/cm^2 reported for a wide range of rivers using a method that involved the agitation of the top 5–10 cm of bed material (Lambert and Walling, 1988; Walling and Quine, 1993; Droppo and Stone, 1994; Walling et al., 1998, López-Tarazón et al., 2011). Most of these studies used a more expansive definition of fine sediment that included fine sand (< 150 μm) and were conducted on reaches with coarser bed material than the mainstem of the lower Salinas River, although the limited amount of work on sandy reaches suggests that they could store a higher proportion of fines than gravel beds (Walling and Quine, 1993). Average annual sediment load estimates based on Inman and Jenkins (1999) and Farnsworth and Milliman (2003) are ~ 30–60 times the amount estimated to have been stored in the reach between S1 and S3, although both studies recognized that many years produced sediment fluxes of this magnitude or less. Thus, the fine sediment potentially stored in the lower Salinas main stem may only exert controls of a small scale relative to decadal- to centennial-scale suspended sediment yield, which is of a similar proportion to the channel storage effects found in another semi-arid catchment (López-Tarazón et al., 2011), but much less than has been found for more maritime climates (Walling et al., 1998).

10.4. The power of antecedent conditions

Unlike bed sediment alone, the hydrologic factors found in this study, though seemingly weak in terms of monotonic correlation coefficients, could have large effects on decadal- to centennial- scale sediment discharge, particularly if influencing the infrequent years responsible for most of the suspended sediment flux through the lower Salinas River. For example, monotonic trends in rating curve residuals against some hydrologic variables show up to 0.5 log unit or greater differences over the domain of variable values, which translates to approximately three times the difference in C_{SS} magnitude (see Fig. 6). As most sediment is transported through the lower Salinas River during a few high discharge days per year, and a few exceptional discharge years over the period of record (Farnsworth and Milliman, 2003), coincidence of discharge events with highly positive or negative hydrologic preconditions could result in large errors in sediment flux estimations that do not take these factors into account. This is particularly true for estimates applying suspended sediment data collected over only one decade to much longer discharge records, such as those of Farnsworth and Milliman (2003) and Inman and Jenkins (1999) for the Salinas River. Moreover, both channel and hydrologic factors could have significant proportional effects on sediment yields during years of lower suspended sediment production and over the range of low to moderate discharge magnitudes commonly found in the lower Salinas, which are of importance in terms of water quality.

11. Conclusions

Suspended sediment rating curves often leave large residual variability in suspended sediment concentration unexplained. Such was the case for the well-studied Salinas River located in a dry summer subtropical climate. Historical and event based hydrological characteristics were found to play a significant role in determining suspended sediment behavior in the lower Salinas. Prolonged drought was found to decrease both sand and fine sediment concentrations. Increased elapsed time since moderate hydrologic events with magnitudes of ~ 10–20 Q_{mean} resulted in increased fine sediment concentration. These moderate flows in the lower Salinas seem to flush the system, depressing subsequent concentrations of fines by exhausting some level of channel and hillslope storage. The importance of channel storage of sediment in the lower Salinas is highlighted by the positive effects of ΔQ_d on fine concentrations, the prevalence of positive hysteresis, the preponderance of incipient flows in the early season and during droughts, and the insensitivity of the system to the dominance of upper Salinas or Arroyo Seco subbasin contributions and hydrologic regime (storm, winter recessional or summer base, and dam release flows) for moderate to low discharge magnitudes. Sand concentrations were found to increase as a result of wet conditions and more recent and larger hydrologic events and to decrease after seasonal scale dry conditions. Recent hydrologic activity also increased sand concentrations, with concentrations increasing when events over a broad range of discharges, from small (0.1 Q_{mean}) to massive (100 Q_{mean}), are more recent. Upper basin and Arroyo Seco sand signatures were also found to persist in the lower Salinas sand suspensions, which also display some evidence of distal basin lag effects relative to the more positive hysteresis

domination of fine sediment. Thus, in-channel contributions to fine suspended sediment behavior is probably not a major control on decadal- to centennial- scale suspended sediment yield from the lower Salinas but may be significant in terms of water quality and annual scale sediment flux. Hydrologic preconditions identified in this study may also significantly influence long-term sediment flux dynamics in the lower Salinas, as they can effect changes in sediment concentration on the order of three times or greater.

The next step in this work is to identify the time dependent pattern of suspended sediment behavior in the lower Salinas and determine if these patterns are influenced by the time dependent behavior of hydrologic conditions and/or land surface change. Further field-based studies of hillslope, channel bed, and bank activity in the lower Salinas and upper basin are also required to directly address the mechanisms behind the antecedent hydrologic effects on suspended sediment behavior found here. Extension of the approach employed here to other systems would benefit greatly from higher resolution water discharge and suspended sediment concentration time series available over longer temporal domains, which are expected to have limited this study from identification of further complexities in the interaction between antecedent conditions and sediment behavior.

Acknowledgements

This research was funded largely by the National Science Foundation under award No. 0628385 and secondarily by the Hydrologic Sciences Graduate Group at the University of California at Davis. This project was also supported by the USDA National

Institute of Food and Agriculture, Hatch project number #CA-D-LAW-7034-H. Any opinions, findings, and conclusions or recommendations expressed in this material are those of the authors and do not necessarily reflect the views of the funding institutions. We thank Peter Barnes, Sarah Greve, Duyen Ho, Olivia Oseguera, Larissa Salaki, and the Elkhorn Slough National Estuarine Research Reserve for laboratory and field assistance, and Rocko Brown for fruitful discussion. This manuscript was significantly improved on the basis of suggestions by Michael Church, one anonymous reviewer, and Editor Richard Marston.

Appendix A. Supplementary material

Supplementary material related to bias calculations and the ANCOVA method for comparing linear regressions can be found in the online version of this article.

References

Andrews, E.D., Antweiler, R.C., Neiman, P.J., Ralph, F.M., 2004. Influence of ENSO on flood frequency along the California coast. Journal of Climate 17(2), 337-348.

Ankers, C., Walling, D.E., Smith, R.P., 2003. The influence of catchment characteristics on suspended sediment properties. Hydrobiologia 494(1-3), 159-167.

Asselman, N.E.M., 1999. Suspended sediment dynamics in a large drainage basin: the River Rhine. Hydrol. Process. 13(10), 1437-1450.

Batalla, R.J., Vericat, D., 2009. Hydrological and sediment transport dynamics of flushing flows: implications for management in large Mediterranean rivers. River Research and Applications 25(3), 297-314.

Benda, L., Dunne, T., 1997. Stochastic forcing of sediment routing and storage in channel networks. Water Resour. Res. 33(12), 2865-2880.

Brasington, J., Richards, K., 2000. Turbidity and suspended sediment dynamics in small catchments in the Nepal Middle Hills. Hydrol. Process. 14(14), 2559-2574.

Brown, C.B., 1943. The Control of Reservoir Silting. U.S. Department of Agriculture, Miscellaneous Publication 21, Washington, D.C.

Brown, W.M., Ritter, J.R., 1971. Sediment Transport and Turbidity in the Eel River Basin, California U.S. Geological Survey Water-Supply Paper 1986, Washington, D.C., 67pp.

Brune, G.M., 1953. Trap efficiency of reservoirs. Trans. Am. Geophys. Union 34, 407-418.

Carson, M.A., Taylor, C.H., Grey, B.J., 1973. Sediment production in a small Appalachian watershed during spring runoff - Eaton-Basin, 1970-1972. Canadian Journal of Earth Sciences 10(12), 1707-1734.

Chakrapani, G.J., 2005. Factors controlling variations in river sediment loads. Curr. Sci. 88(4), 569-575.

Cleveland, W.S., 1979. Robust locally weighted regression and smoothing scatterplots. J. Am. Stat. Assoc. 74, 829-836.

Cleveland, W.S., Devlin, S.J., 1988. Locally weighted regression: an approach to regression analysis by local fitting. J. Am. Stat. Assoc. 83(403), 596-610.

Constantine, J.A., Pasternack, G.B., Johnson, M.L., 2005. Logging effects on sediment flux observed in a pollen-based record of overbank deposition in a northern California catchment. Earth Surf. Process. Landf. 30(7), 813-821.

de Vente, J., Poesen, J., Arabkhedri, M., Verstraeten, G., 2007. The sediment delivery problem revisited. Prog. Phys. Geogr. 31(2), 155-178.

Droppo, I.G., Stone, M., 1994. In-channel surficial fine-grained sediment laminae 1. Physical characteristics and formational processes. Hydrol. Process. 8(2), 101-111.

Estrany, J., Garcia, C., Batalla, R.J., 2009. Groundwater control on the suspended sediment load in the Na Borges River, Mallorca, Spain. Geomorphology 106(3-4), 292-303.

Farnsworth, K.L., Milliman, J.D., 2003. Effects of climatic and anthropogenic change on small mountainous rivers: the Salinas River example. Glob. Planet. Change 39(1-2), 53-64.

Farnsworth, K.L., Warrick, J.A., 2007. Sources, Dispersal, and Fate of Fine Sediment Supplied to Coastal California. U.S. Geological Survey Scientific Investigations Report 2007–5254, Washington, D.C., 77pp.

Ferguson, R.I., 1986. River loads underestimated by rating curves. Water Resour. Res. 22(1), 74-76.

Gao, P., Pasternack, G.B., 2007. Dynamics of suspended sediment transport at field-scale drain channels of irrigation-dominated watersheds in the Sonoran Desert, southeastern California. Hydrol. Process. 21(16), 2081-2092.

Gao, P., Josefson, M., 2012. Event-based suspended sediment dynamics in a central New York watershed. Geomorphology 139, 425-437.

Garcia, M., Parker, G., 1991. Entrainment of bed sediment into suspension. J. Hydraul. Eng.-ASCE 117(4), 414-435.

Gonzalez-Hidalgo, J.C., Batalla, R.J., Cerda, A., de Luis, M., 2010. Contribution of the

largest events to suspended sediment transport across the USA. Land Degradation & Development 21(2), 83-91.

Gray, A.B., Pasternack, G.B., Watson, E.B., 2010. Hydrogen peroxide treatment effects on the particle size distribution of alluvial and marsh sediments. Holocene 20(2), 293-301.

Heidel, S.G., 1956. The progressive lag of sediment concentration with flood waves. Trans. Am. Geophys. Union 37, 56–66.

Heinemann, H.G., 1981. A new sediment trap efficiency curve for small reservoirs. Water Resour. Bull. 17(5), 825-830.

Heinemann, H.G., 1984. Reservoir trap efficiency. In: Hadley, R.F., Walling, D.E., (Eds.), Erosion and Sediment Yield: Some Methods of Measurement and Modelling. GeoBooks, Norwich, CT, pp. 201–218.

Helsel, D.R., Hirsch, R.M., 2002. Statistical Methods in Water Resources—Hydrologic Analysis and Interpretation. U.S. Geological Survey Techniques of Water-Resources Investigations book 4, chap. A3, Washington, DC, 510 pp.

Hill, P.S., Nowell, A.R.M., Jumars, P.A., 1988. Flume evaluation of the relationship between suspended sediment concentration and excess boundary shear-stress. J. Geophys. Res.-Oceans 93(C10), 12499-12509.

Horowitz, A.J., 2003. An evaluation of sediment rating curves for estimating suspended sediment concentrations for subsequent flux calculations. Hydrol. Process. 17(17), 3387-3409.

Hudson, P.F., 2003. Event sequence and sediment exhaustion in the lower Panuco basin, Mexico. Catena 52(1), 57-76.

Inman, D.L., Jenkins, S.A., 1999. Climate change and the episodicity of sediment flux of small California rivers. J. Geol. 107(3), 251-270.

Kale, V.S., Hire, P.S., 2004. Effectiveness of monsoon floods on the Tapi River, India: role of channel geometry and hydrologic regime. Geomorphology 57(3-4), 275-291.

Kelsey, H.M., 1980. A sediment budget and an analysis of geomorphic process in the Van-Duzen River basin, north coastal California, 1941-1975 - summary. Geol. Soc. Am. Bull. 91(4), 190-195.

Korup, O., 2012. Earth's portfolio of extreme sediment transport events. Earth-Science Reviews 112(3-4), 115-125.

Lambert, C.P., Walling, D.E., 1988. Measurement of channel storage of suspended sediment in a gravel-bed river. Catena 15(1), 65-80.

Lana-Renault, N., Regues, D., Marti-Bono, C., Begueria, S., Latron, J., Nadal, E., Serrano, P., Garcia-Ruiz, J.M., 2007. Temporal variability in the relationships between precipitation, discharge and suspended sediment concentration in a small Mediterranean mountain catchment. Nord. Hydrol. 38(2), 139-150.

Langbein, W.B., Schumm, S.A., 1958. Yield of sediment in relation to mean annual precipitation. Trans. Am. Geophys. Union 39, 1076-1084.

Larsen, P.V., 2003. ST111: Regression analysis and analysis of variance. http://statmaster.sdu.dk/courses/st111/ (last accessed: 12/2012).

Lenzi, M.A., Marchi, L., 2000. Suspended sediment load during floods in a small stream of the Dolomites (northeastern Italy). Catena 39(4), 267-282.

Leopold, L.B., Maddock, T.J., 1953. Hydraulic Geometry of Stream Channels and Some Physiographic Implications. U.S. Geological Survey Professional Paper 252,

Washington, D.C., 55 pp.

López-Tarazón, J.A., Batalla, R.J., Vericat, D., Balasch, J.C., 2010. Rainfall, runoff and sediment transport relations in a mesoscale mountainous catchment: the River Isabena (Ebro basin). Catena 82(1), 23-34.

López-Tarazón, J.A., Batalla, R.J., Vericat, D., 2011. In-channel sediment storage in a highly erodible catchment: the River Isabena (Ebro Basin, southern Pyrenees). Z. Geomorphol 55(3), 365-382.

Madej, M.A., Ozaki, V., 1996. Channel response to sediment wave propagation and movement, Redwood Creek, California, USA. Earth Surf. Proc. Land (21), 911-927.

Mano, V., Nemery, J., Belleudy, P., Poirel, A., 2009. Assessment of suspended sediment transport in four alpine watersheds (France): influence of the climatic regime. Hydrol. Process 23(5), 777-792.

McCulloch, M., Fallon, S., Wyndham, T., Hendy, E., Lough, J., Barnes, D., 2003. Coral record of increased sediment flux to the Great Barrier Reef since European settlement. Nature 421(6924), 727-730.

McLeod, A.I., 2011. Package 'Kendall.' Kendall rank correlation and Mann-Kendall trend test. CRAN. Classification/MSC 62M10, 91B84. http://www.stats.uwo.ca/faculty/aim. (last accessed: 12/2012).

Meade, R.H., Yuzyk, T.R., Day, T.J. (Eds.), 1990. Movement and storage of sediment in rivers of the United States and Canada. In: Surface Water Hydrology, The Geology of North America 0-1. Geol. Soc. of Am., Boulder, CO. 255-280 pp.

Mehta, A.J., Hayter, E.J., Parker, W.R., Krone, R.B., Teeter, A.M., 1989. Cohesive sediment transport. 1. Process description. J. Hydraul. Eng.-ASCE 115(8), 1076-

1093.

Milliman, J.D., Syvitski, J.P.M., 1992. Geomorphic/tectonic control of sediment discharge to the ocean: the importance of small mountainous rivers. The Journal of Geology 100(5), 525-544.

Neagley, J.P., Robert, T., O'Brien, J., 1990. Market allocation of agricultural water resources in the Salinas River valley. Masters thesis, Naval Postgraduate School, Monterey, CA, 96 pp.

Nutter, E.H., 1901. Sketch of the geology of the Salinas Valley, California. J. Geol. 9(4), 330-336.

Oeurng, C., Sauvage, S., Sanchez-Perez, J.M., 2010. Dynamics of suspended sediment transport and yield in a large agricultural catchment, southwest France. Earth Surf. Process. Landf. 35(11), 1289-1301.

Pasternack, G.B., Brush, G.S., Hilgartner, W.B., 2001. Impact of historic land-use change on sediment delivery to a Chesapeake Bay subestuarine delta. Earth Surf. Process. Landf. 26(4), 409-427.

Paustian, S.J., Beschta, R.L., 1979. The suspended sediment regime of an Oregon coast range stream. Wat. Res. Bull. 15(1), 144-154.

Poesen, J.W.A., Hooke, J.M., 1997. Erosion, flooding and channel management in Mediterranean environments of southern Europe. Prog. Phys. Geogr. 21(2), 157-199.

R Development Core Team, 2012. R: A Language and Environment for Statistical Computing. R Foundation for Statistical Computing, Vienna, Austria. ISBN 3-900051-07-0, http://www.R-project.org/ (last accessed: 12/2012).

Rosenberg, L.I., Joseph, J.C., 2009. Map of the Rinconada and Reliz Fault Zones, Salinas River Valley, California: U.S. Geological Survey Scientific Investigations Map 3059, scale 1:250,000 with pamphlet, http://pubs.usgs.gov/sim/3059/ (last accessed: 12/2012).

Rouse, H., 1937. Modern conceptions of the mechanics of fluid turbulence. Transactions of the American Society of Civil Engineers 102, 463-541.

Rouse, H. 1938. Fluid Mechanics for Hydraulic Engineers. Dover, New York, 422 pp.

Sadeghi, S.H.R., Mizuyama, T., Miyata, S., Gomi, T., Kosugi, K., Fukushima, T., Mizugaki, S., Onda, Y., 2008. Development, evaluation and interpretation of sediment rating curves for a Japanese small mountainous reforested watershed. Geoderma 144(1-2), 198-211.

Shi, Y.L., Yang, W., Ren, M.E., 1985. Hydrological characteristics of the Changjiang and its relation to sediment transport to the sea. Cont. Shelf Res. 4(1-2), 5-15.

Syvitski, J.P., Morehead, M.D., Bahr, D.B., Mulder, T., 2000. Estimating fluvial sediment transport: the rating parameters. Water Resour. Res. 36(9), 2747-2760.

Tena, A., Batalla, R.J., Vericat, D., López-Tarazón, J.A., 2011. Suspended sediment dynamics in a large regulated river over a 10-year period (the lower Ebro, NE Iberian Peninsula). Geomorphology 125(1), 73-84.

Thompson, J.G., Reynolds, R., 2002. Cultural evolution and water management in the Salinas River valley. J. Am. Water Resour. Assoc. 38(6), 1661-1677.

U.S. Geological Survey National Water Information System (USGS NWIS), 2013 http://waterdata.usgs.gov/nwis/sw (last accessed: 03/2013).

Walling, D.E., 1977. Assessing accuracy of suspended sediment rating curves for a

small basin. Water Resour. Res. 13(3), 530-538.

Walling, D.E., Moorehead, P.W., 1987. Spatial and temporal variation of the particle-size characteristics of fluvial suspended sediment. Geografiska Annaler Series A, Phys. Geogr. 69(1), 47-59.

Walling, D.E., Quine, T.A., 1993. Using Chernobyl-derived fallout radionuclides to investigate the role of downstream conveyance losses in the suspended sediment budget of the River Severn, United-Kingdom. Phys. Geogr. 14(3), 239-253.

Walling, D.E., Owens, P.N., Leeks, G.J.L., 1998. The role of channel and floodplain storage in the suspended sediment budget of the River Ouse, Yorkshire, UK. Geomorphology 22(3-4), 225-242.

Warrick, J.A., Rubin, D.M., 2007. Suspended-sediment rating curve response to urbanization and wildfire, Santa Ana River, California. J. Geophys. Res.-Earth Surf. 112(F2), 1-15.

Warrick, J.A., Mertes, L.A.K., 2009. Sediment yield from the tectonically active semiarid Western Transverse Ranges of California. Geol. Soc. Am. Bull. 121(7-8), 1054-1070.

Warrick, J.A., Hatten, J.A., Pasternack, G.B., Gray, A.B., Goni, M.A., Wheatcroft, R.A., 2012. The effects of wildfire on the sediment yield of a coastal California watershed. Geol. Soc. Am. Bull. 124(7-8), 1130-1146.

Warrick, J.A., Madej, M.A., Goni, M.A, Wheatcroft, R.A., 2013. Trends in the suspended-sediment yields of coastal rivers of northern California, 1955–2010. Journal of Hydrology 489, 108-123.

Watson, E.B., Pasternack, G.B., Gray, A.B., Goni, M., Woolfolk, A.M., 2013. Particle

size characterization of historic sediment deposition from a closed estuarine lagoon, central California. Estuar. Coast. Shelf Sci. 126, 23-33.

Wheatcroft, R.A., Goni, M.A., Hatten, J.A., Pasternack, G.B., Warrick, J.A., 2010. The role of effective discharge in the ocean delivery of particulate organic carbon by small, mountainous river systems. Limnol. Oceanogr. 55(1), 161-171.

Williams, G.P., 1989. Sediment concentration versus water discharge during single hydrologic events in rivers. J. Hydrol. 111(1-4), 89-106.

Willis, C.M., Griggs, G.B., 2003. Reductions in fluvial sediment discharge by coastal dams in California and implications for beach sustainability. J. Geol. 111(2), 167-182.

Winterwerp, J.C., Cornelisse J.M., Kuijper, C., 1990. Parameters to characterize natural muds. In: Abstract Volume, Int. Workshop on Cohesive Sediments, Brussels. KBIN, Brussels, 103-105 pp.

Wischmeier, W.H., Smith, D.D., 1978. Predicting Rainfall Erosion Losses: A Guide to Conservation Planning. USDA/ Purdue Agricultural Experiment Station.

Table 1

Gage stations and Salinas River reaches

ID[a]	USGS gage name	USGS gage #	SS data	Record interval of Q_d (water years)	Drainage area (km)	Reach	Distance[b] (km)
S1	*Salinas R. near Spreckels*	11152500	yes	1931 - 2011	10,764	S1 to S2	23.51
S2	*Salinas R. near Chualar*	11152300	yes	1976 - 2011	10,469	S2 to confluence	28.41
S3	*Salinas R. at Soledad*	11151700	no	1969 - 2011	9,228	Confluence to S3	1.36
S4	*Salinas R. near Bradley*	11150500	no	1948 - 2011	6,566	S3 to S4	84.69
A1	*Arroyo Seco below Reliz Creek*	11152050	yes	1994 - 2011	787	Confluence to A1	1.74
A2	*Arroyo Seco near Soledad*	11152000	no	1962 - 1986	632	A1 to A2	17.28
A3	*Arroyo Seco near Greenfield*	11151870	yes	1901 - 2011	113	A2 to A3	24.79

[a]Identification code for this study.

[b]River distance measure by following approximate thalweg.

Table 2

Hydrologic variables tested for correlation with discharge-corrected suspended sediment concentrations[a]

Hydrologic variables	Unit	Index	Hydrologic argument	Temporal criteria	Temporal window
ΔQ_d	m^3/s	event conditions	$Q_{dt} - Q_{d(t-1)}$	n/a	1 day
Current annual water yield	10^5 m^3	basin wetness	ΣWy	year = sampling year	1 water year
Previous annual water yield	10^5 m^3	basin wetness	ΣWy	year = sampling year -1	1 water year
Current annual precipitaton	cm	basin wetness	n/a	year = sampling year	1 water year
Previous annual precipitaton	cm	basin wetness	n/a	year = sampling year	1 water year
$\Sigma Q_{0.1}$	days	seasonality, basin aridity	$Q_d \leq 0.1$ m^3/s	sum of days	10 to 2000 days
Q_j *time*	days	event history	$Q_d \leq Q_j$	elapsed time	1930-2011

[a]Discreet variables: ΔQ_d = the difference in Q_d from the day before sampling to the day of sampling. Collections of variables: $\Sigma Q_{0.1}$ = sum of days where daily discharge (Q_d) is less than or equal to 0.1 m^3/s, with individual variables defined by days between the last Q_d of a given magnitude j and the date of sample, with individual variables defined by values of j from 1 to 1000 m^3/s in 1-m^3/s steps.

Table 3

Mann-Kendall trend analysis[a]

Variable	Fines		Sand	
	Tau	2-sided *P* -value	*Tau*	2-sided *P* -value
ΔQ_d	0.081	0.03	0.01	0.84
Precipitation, same year	0.026	0.48	0.11	0.01
Precipitation, previous year	-0.059	0.12	0.17	6.2E-05
Water yield, same year	0.014	0.71	0.11	9.5E-03
Water yield, previous year	-0.002	0.95	0.18	4.2E-05
$\Sigma Q_{0.1}$ *(10 day window)*	0.025	0.56	-0.19	1.5E-04
$\Sigma Q_{0.1}$ *(100 day window)*	0.042	0.27	-0.29	9.7E-11
$\Sigma Q_{0.1}$ *(500 day window)*	-0.036	0.33	-0.21	9.6E-07
$\Sigma Q_{0.1}$ *(1200 day window)*	-0.08	0.03	-0.13	1.9E-03
$\Sigma Q_{0.1}$ *(2000 day window)*	-0.111	2.6E-03	-0.21	6.5E-07
Q_1 *time*	-0.103	0.01	-0.18	1.2E-04
Q_{100} *time*	0.169	6.0E-06	-0.15	6.6E-04
Q_{200} *time*	0.117	1.5E-03	-0.18	3.2E-05
Q_{400} *time*	-0.067	0.07	-0.28	9.0E-11

[a]All results are Mann-Kendall (MK) trend analyses with dependent variables as ($\log C_{SSf} \sim \log Q$) or ($\log C_{SSs} \sim \log Q$) LOESS residuals against hydrologic predictor variables.

Table 4

ANCOVA results[a]

Regression pair	n	Coincidence	Parallelism	Offset
Rising,falling (fines)	97, 139	***	parallel	equivalent
Rising, falling (sand)	61, 107	coincident	parallel	equivalent
Storm, winter recessional, summer base	27, 31, 69	coincident	parallel	equivalent
Storm, winter recessional	122, 38	coincident	parallel	equivalent
Upper Salinas, Arroyo Seco (fines)	118, 61	coincident	parallel	equivalent
Upper Salinas, Arroyo Seco (sand)	99, 24	*	**	*
S1, S2 (< 2 μm clay)	50/38	coincident	parallel	equivalent
S1, S2 (2 to 4 μm clay)	50/37	coincident	parallel	equivalent
S1, S2 (4 to 8 μm silt)	49/38	coincident	parallel	equivalent
S1, S2 (8 to 16 μm silt)	47/37	coincident	parallel	equivalent
S1, S2 (16 to 31 μm silt)	42/32	coincident	parallel	equivalent
S1, S2 (31 to 62.5 μm sand)	42/33	coincident	parallel	equivalent
S1, S2 (62.5 to 125 μm sand)	76/45	*	parallel	equivalent
S1, S2 (125 to 250 μm sand)	86/51	*	parallel	equivalent
S1, S2 (250 to 500 μm sand)	69/46	coincident	parallel	equivalent
S1, S2 (500 to 1000 μm sand)	18/18	coincident	parallel	equivalent
S1, S2 (125 to 2000 μm sand)	87/51	*	parallel	equivalent

[a]Rising and falling refer to hydrographic position. Storm, winter recessional, and summer base flow are hydrologic regime subgroups. Upper Salinas and Arroyo Seco refer to subgroups defined by dominant subbasin contribution to flow. S1 is the Salinas mainstem gauging station at Spreckels, S2 is the Salinas mainstem gauging station at Chualar. n = number of samples by subgroup. The results of coincident, parallel, and offset equivalent (respectively) are identified as such, and significant results to the contrary are indicated as: * P-value < 0.05, ** P-value < 0.01, *** P-value < 0.001.

Table 5

Hydraulic geometry of Salinas stations[a]

	Width	Depth	Velocity		
Site	*b*	*f*	*m*	*b* /*f* ratio	*m* /*f* ratio
S1	0.49	0.34	0.17	1.44	0.48
S2	0.44	0.35	0.21	1.26	0.59
S3	0.50	0.34	0.16	1.50	0.48
A1	0.44	0.25	0.30	1.75	1.20

[a]Slope coefficients of power functions relating width, depth, and velocity to discharge are *b, f* , and *m,* respectively.

Figure Captions

Fig. 1. The Salinas River watershed drains a portion of the northern California Coast Ranges into Monterey Bay. Dark gray areas represent the watersheds of the dammed reservoirs (from S to N) Santa Margarita Lake, Lake Nacimiento and Lake San Antonio completed in 1941, 1961, and 1965, respectively. S1–S4 and A1–A3 are USGS hydrologic gaging stations located on the Salinas and Arroyo Seco rivers, respectively (see Table 1 for details). BGS, SAP, and PSV are the NOAA precipitation gages, Big Sur State Park, Salinas No. 2, and Priest Valley, respectively.

Fig. 2. Lower Salinas suspended sediment samples collected by the (A) USGS and (B) the authors (UCD) at stations S1 and S2, which correspond to the USGS gaging stations #11152500 (Salinas Spreckels) and #11152300 (Salinas Chualar), respectively.

Fig. 3. Suspended sediment rating curves and residuals from lower Salinas River samples. Fine suspended sediment concentration (A) and sand suspended sediment concentration (B) plotted with simple linear regression curves in dashed lines and LOESS curves in solid lines. Concomitant linear regression rating curve residuals for (C) fines and (D) sand are followed by LOESS rating curve residuals (E) and (F) for fine and sands respectively, and sequentially summed residuals over the discharge regime (G) and (H).

Fig. 4. Mann-Kendall analysis of monotonic trends in lower Salinas for (A) fine and (B) sand-sized suspended sediment LOESS rating curve residuals in relation to the sum of days with $Q_d \leq 0.1$ m^3/s over summation windows of 1–2000 days. Instability in the

response of (A) fine residuals to variables produced from shorter windows was followed by consistently negative trends for all summation windows above ~ 1150 days or ~ 3 years, as indicated by shading. The response of (B) sand residuals was stable and negative across the entire range of summation window lengths.

Fig. 5. Mann-Kendall analysis test results for monotonic trends in lower Salinas (A) fine, and (B) sand-sized suspended sediment LOESS rating curve residuals in relation to elapsed time since the last hydrologic event of a given size (Q_j). Shaded bars indicate intervals of hydrologic event values that yielded significant monotonic trends in the rating curve residuals. (A) Very low and high discharges produced significant, negative trends in fine rating curve residuals with increasing elapsed time between events, while moderately large events affected positive trends as elapsed time increased. Trends in sand-sized rating curve residuals were negative and significant for all magnitudes of Q_j except for the range of ~ 20–50 m^3/s.

Fig. 6. Plots of fine (A–F) and sand (G–L) LOESS rating curve residuals against different variable states for $\sum Q_{0.1}$ (A–C, G–I) and Q_j *time* (D–F, J–L). (A–C) Fine residual response to $\sum Q_{0.1}$ does not appear to be monotonic for the variables shown, whereas all other plots appear to exhibit monotonic behavior.

Fig. 7. Lower Salinas subgroup sediment rating curves defined by hydrographic and hydrologic criteria: (A) fine, and (B) sand-sized sediment by hydrographic position (samples from rising or falling limbs of the hydrograph), and (C–D) hydrologic modes (storm, winter recessional, and base flow). Discharge ranges are limited to shared ranges for the hydrologic mode rating curves. The difference between (A) fine rising and

falling limb samples was significant at the $p < 0.05$ level. The differences between the (B) sand-sized rising and falling limb samples and (C–D) hydrologic mode subgroups were not significant.

Fig. 8. Diagrams of all fine suspended sediment hysteresis events identified from the lower Salinas USGS and UCD data sets plotted in log-log scale and organized by discharge magnitude of the peak event flow. Rising flows progress in temporal sequence from left to right (low to high discharge), while falling flows progress from right to left (high to low discharge). Positive or clockwise hysteresis occurs when rising limb flows have higher suspended sediment concentrations than falling limb flows. Negative or counter-clockwise hysteresis occurs when falling limb samples have higher suspended sediment concentrations than rising limb flows. Mixed hysteresis events display each of these patterns over different ranges of discharge magnitude. Sample were collected from the lower Salinas at location S1 (USGS Spreckels gage) during events plotted in (A), (B), (D) and (F-H), and at S2 (USGS Chualar gage) for (C) and (E). Samples (C) and (E) were collected by UCD, all others by the USGS. Event date ranges are as follows: (A) 12/10–14/1974, (B) 12/27/1971–1/1/1972, (C) 2/25–26/2010, (D) 1/11–17/1970, (E) 1/20–25/2010, (F) 1/5–25/1974, (G) 2/10–22/1973, (H) 2/8–27/1978.

Fig. 9. Paired plots of fine and sand-sized C_{SS} behavior over the course of rising and falling Q magnitudes during lower Salinas hydrologic events. Rising limb samples progress in temporal sequence from left to right (low to high Q), and falling limb samples from right to left (high to low Q). All samples were collected from the lower Salinas at location S1 (USGS Spreckels gage). Event date ranges are as follows: (A,B)

12/27/1971–1/1/1972, (C,D) 1/11–17/1972, (E,F) 2/10–22/1973, (G,H) 4/2–11/1974, (I,J) 2/8–10/1973, (K,L) 2/8–27/1978, (M,N) 1/5–25/1974.

Fig. 10. (A) Fine and (B) sand-sized sediment in the lower Salinas linear regression rating curves sub-divided by subbasin water provenance (upper Salinas and Arroyo Seco). (A) Fine sediment behavior by water provenance was statistically coincident, while (B) sand behavior differed in terms of rating curve slope and offset.

Fig. 11. LOESS rating curves fitted to lower Salinas suspended sediment by (A) texture class (clay, silt, and sand), (B) clay, (C) silt, and (D, E) sand particle size ranges. All LOESS curves were computed for combined stations S1 and S2 data sets, except for sand particle sizes 62.5–125 and 125–250 μm, as log-linear rating curves for these ranges were significantly different between stations.

Fig. 12. Lower Salinas average suspended sediment particle size distributions for stations S1 (A, C, E, G, I) and S2 (B, D, F, H, J, L) by discharge magnitude, and channel beds (K, L). Distributions were calculated from LOESS curves plotted for each particle size range, and by station when log-linear regressions indicated significant differences in behavior between stations (62.5–125 and 125–250 μm) (see Fig. 11). All data derived from USGS sources.

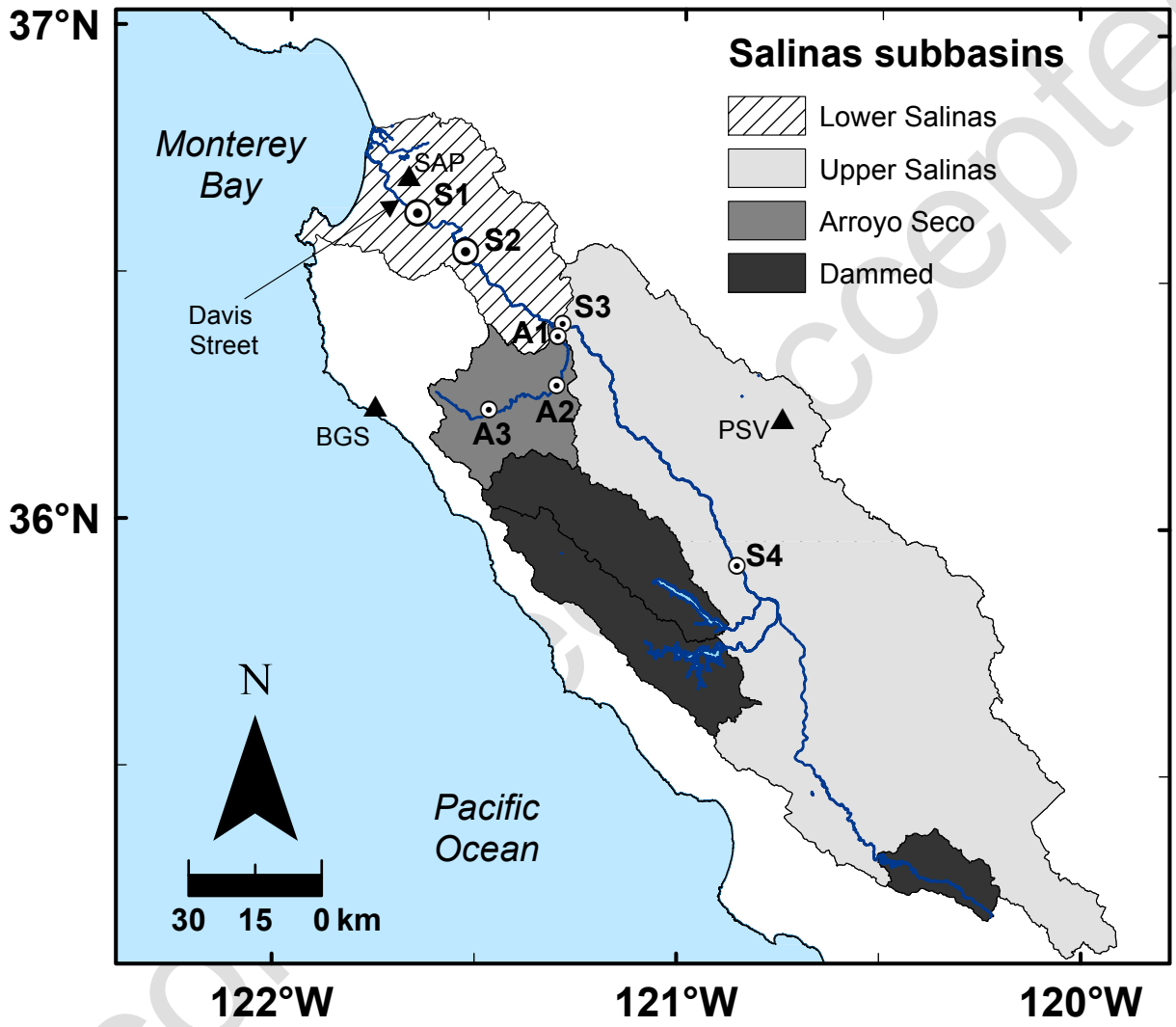

Figure 1.

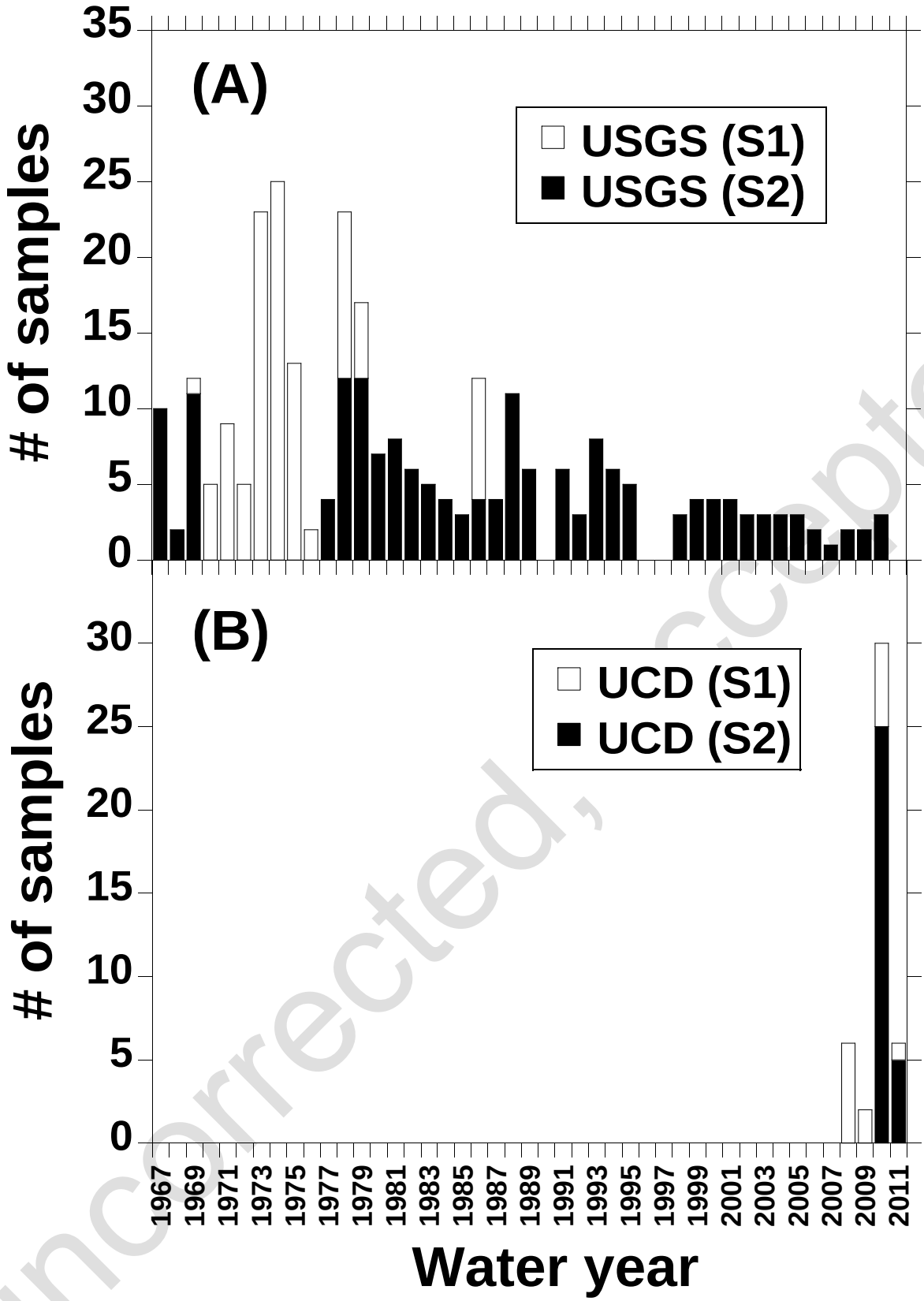

Figure 2.

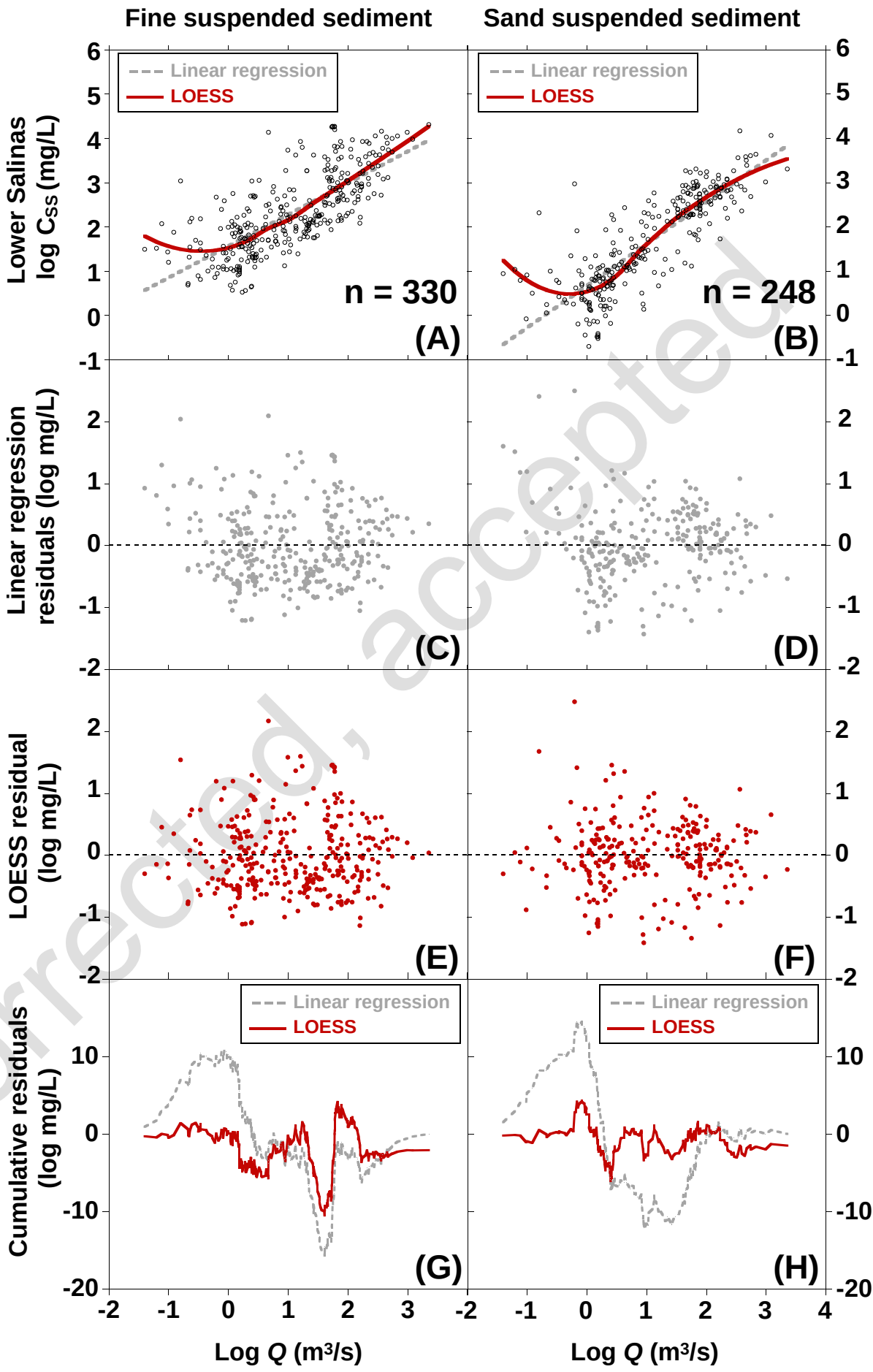

Figure 3.

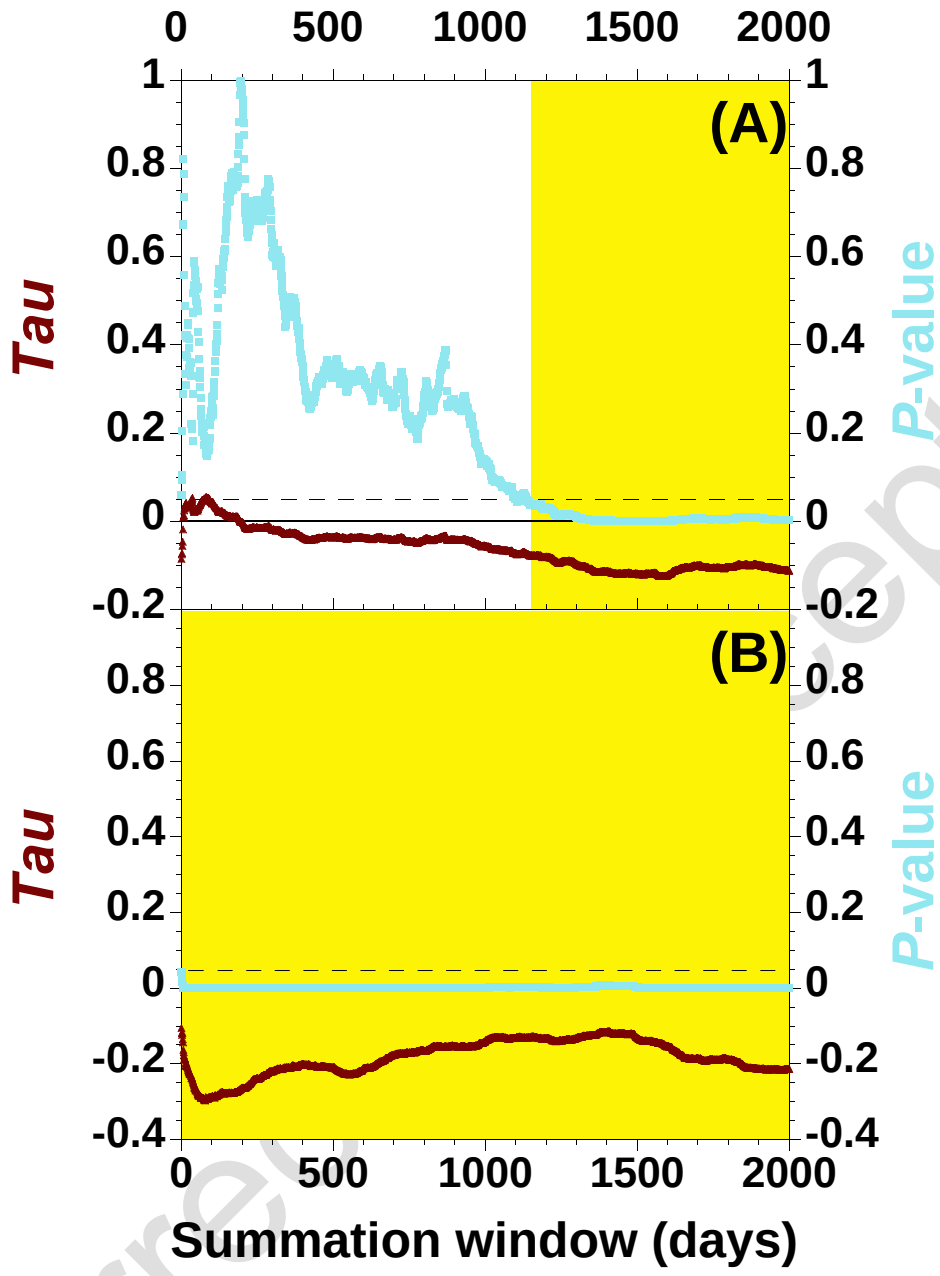

Figure 4.

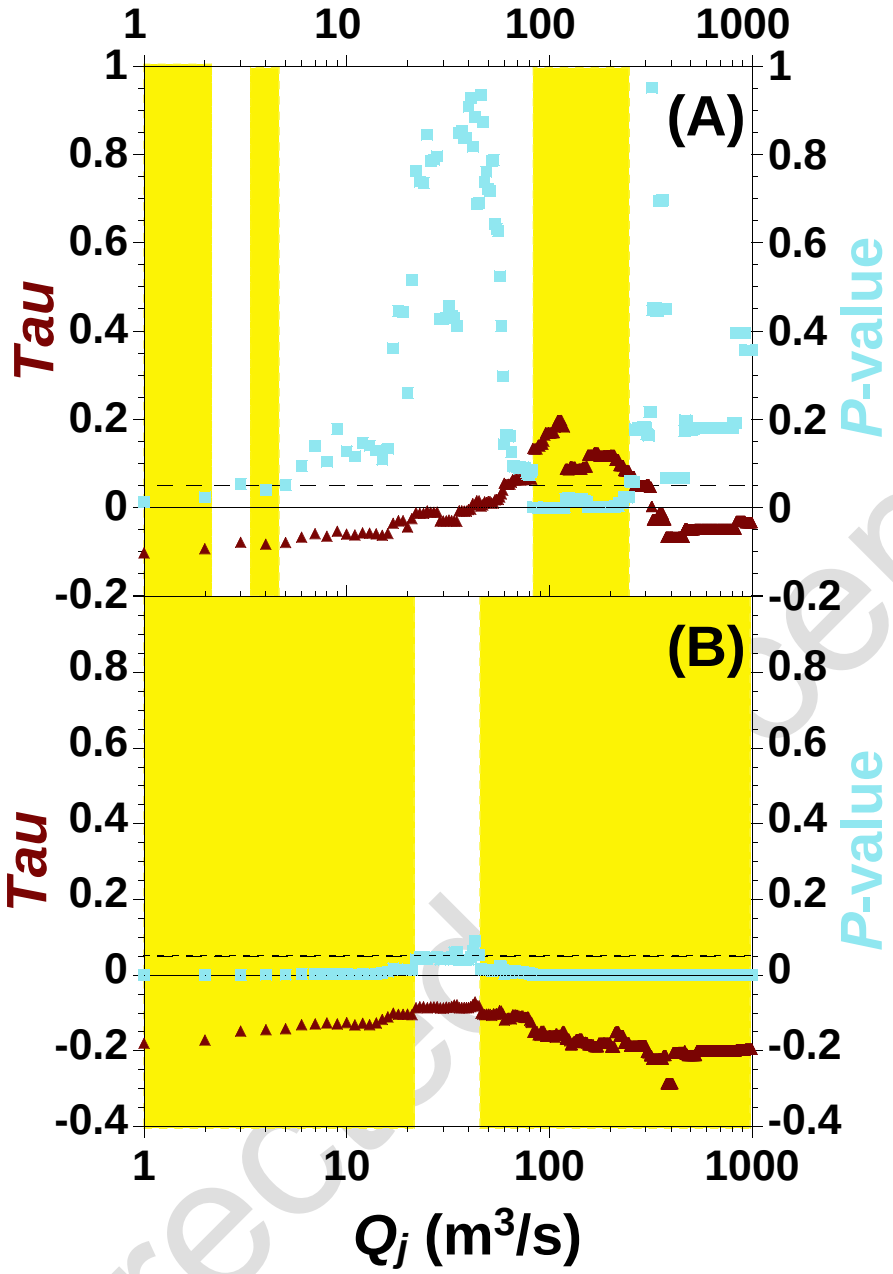

Figure 5.

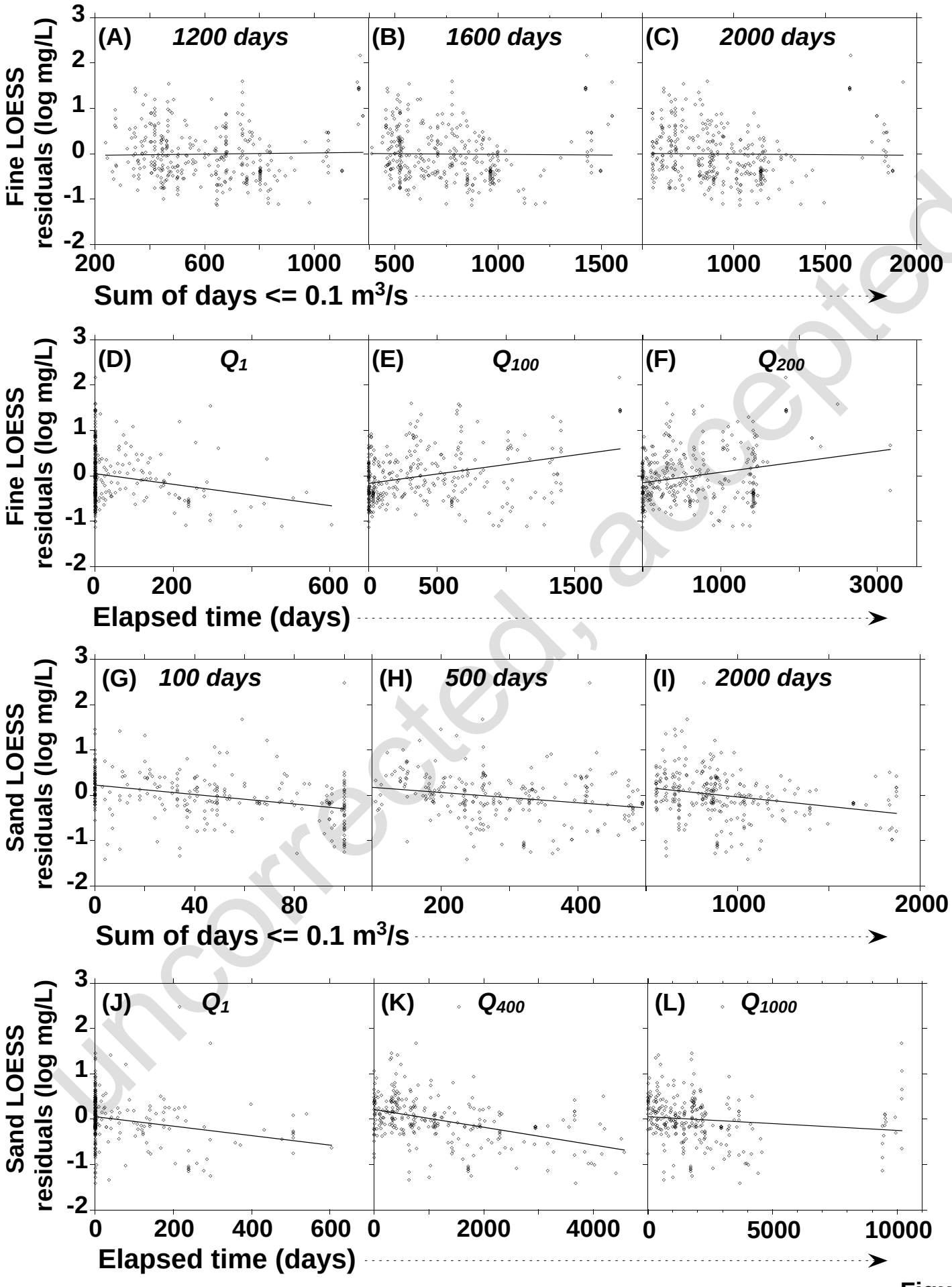

Figure 6.

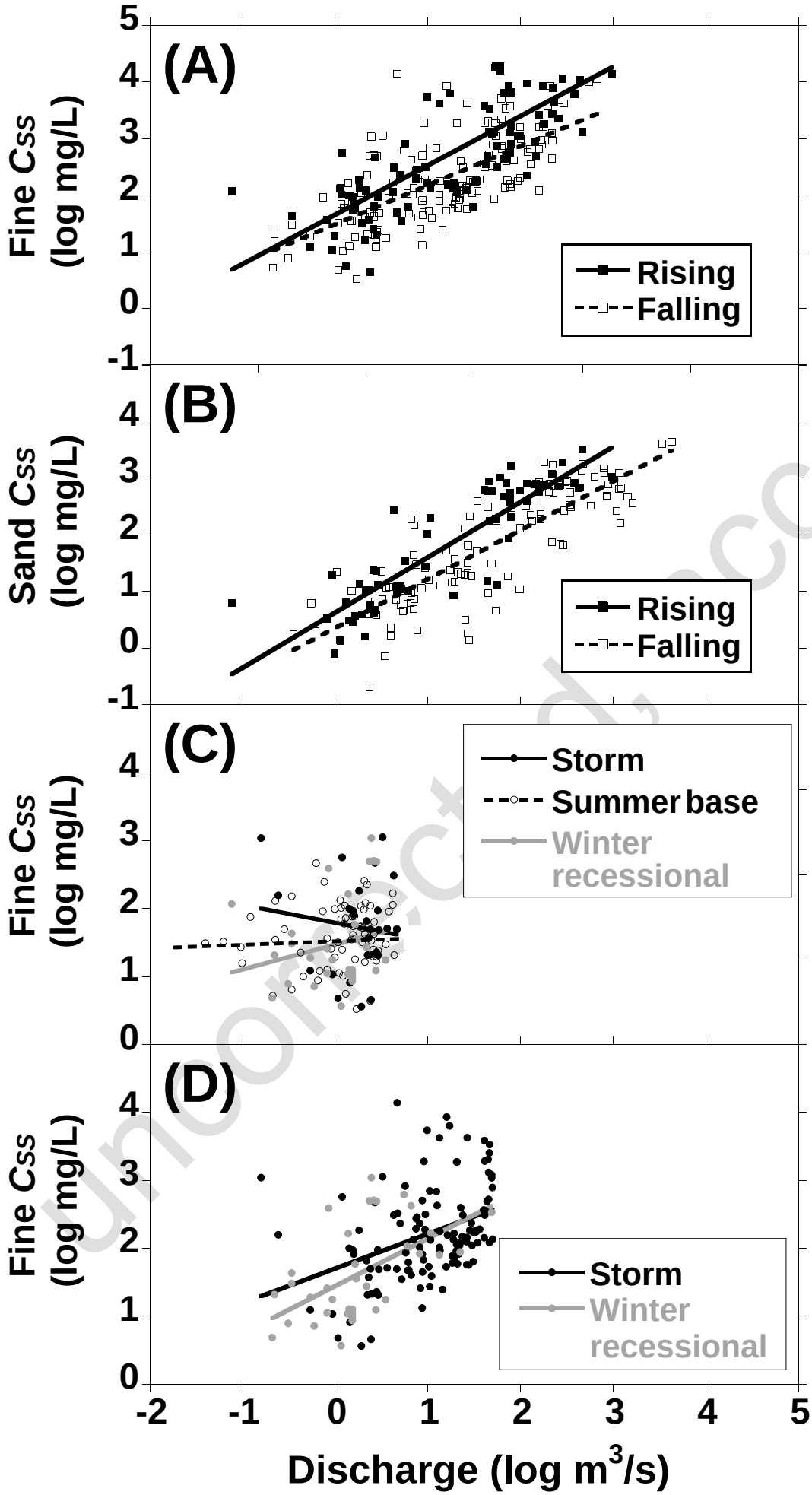

Figure 7.

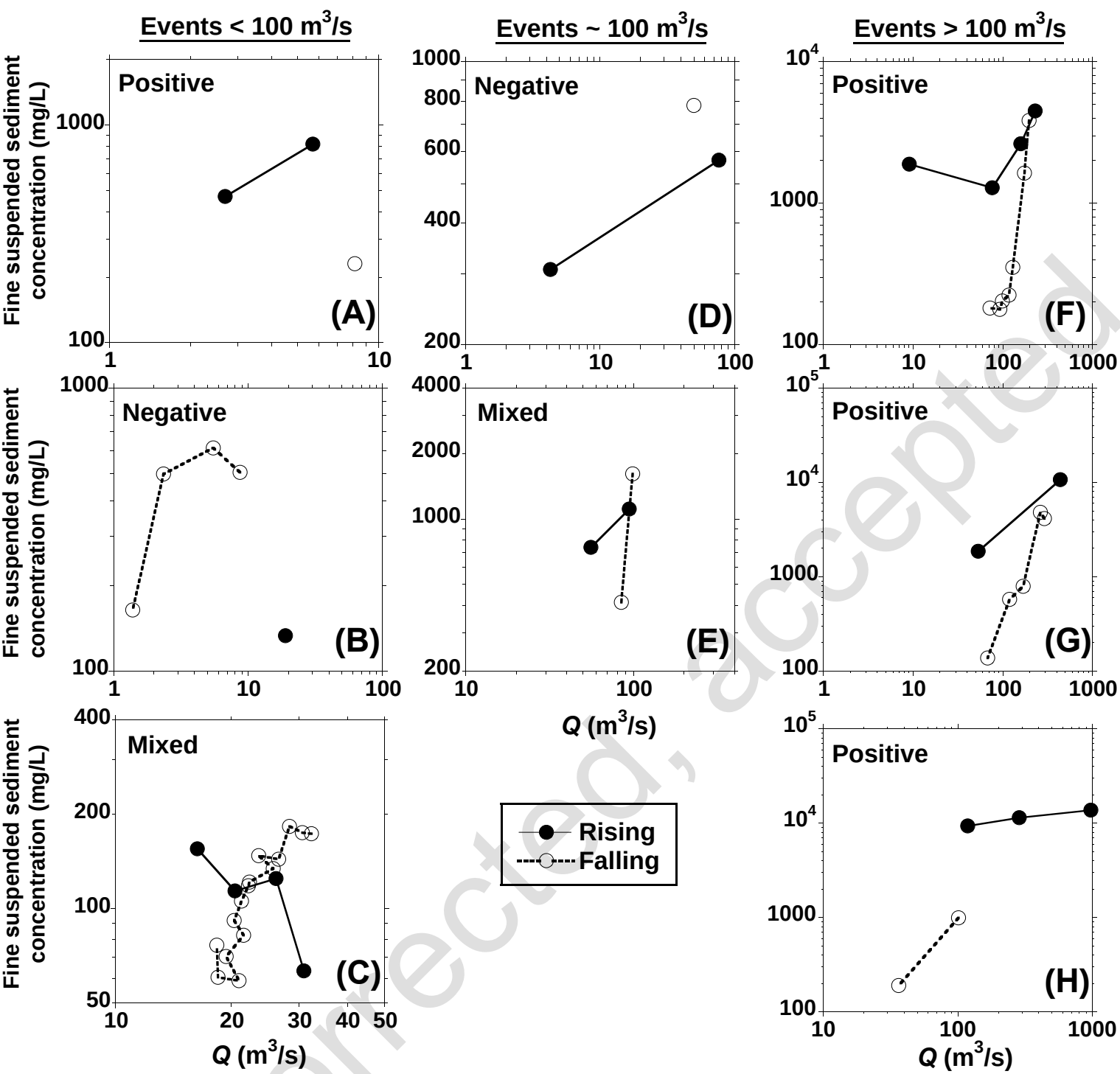

Figure 8.

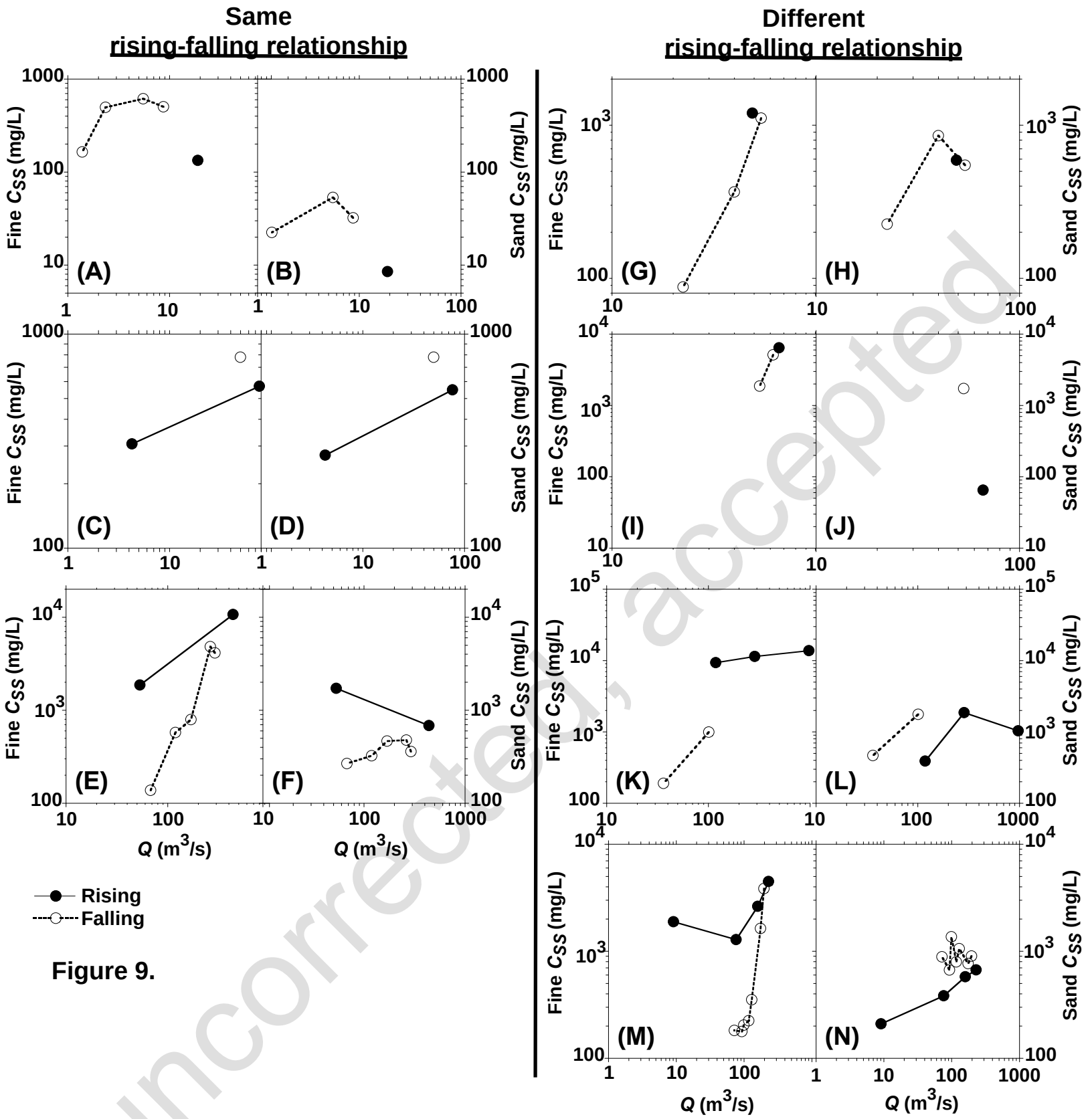

Figure 9.

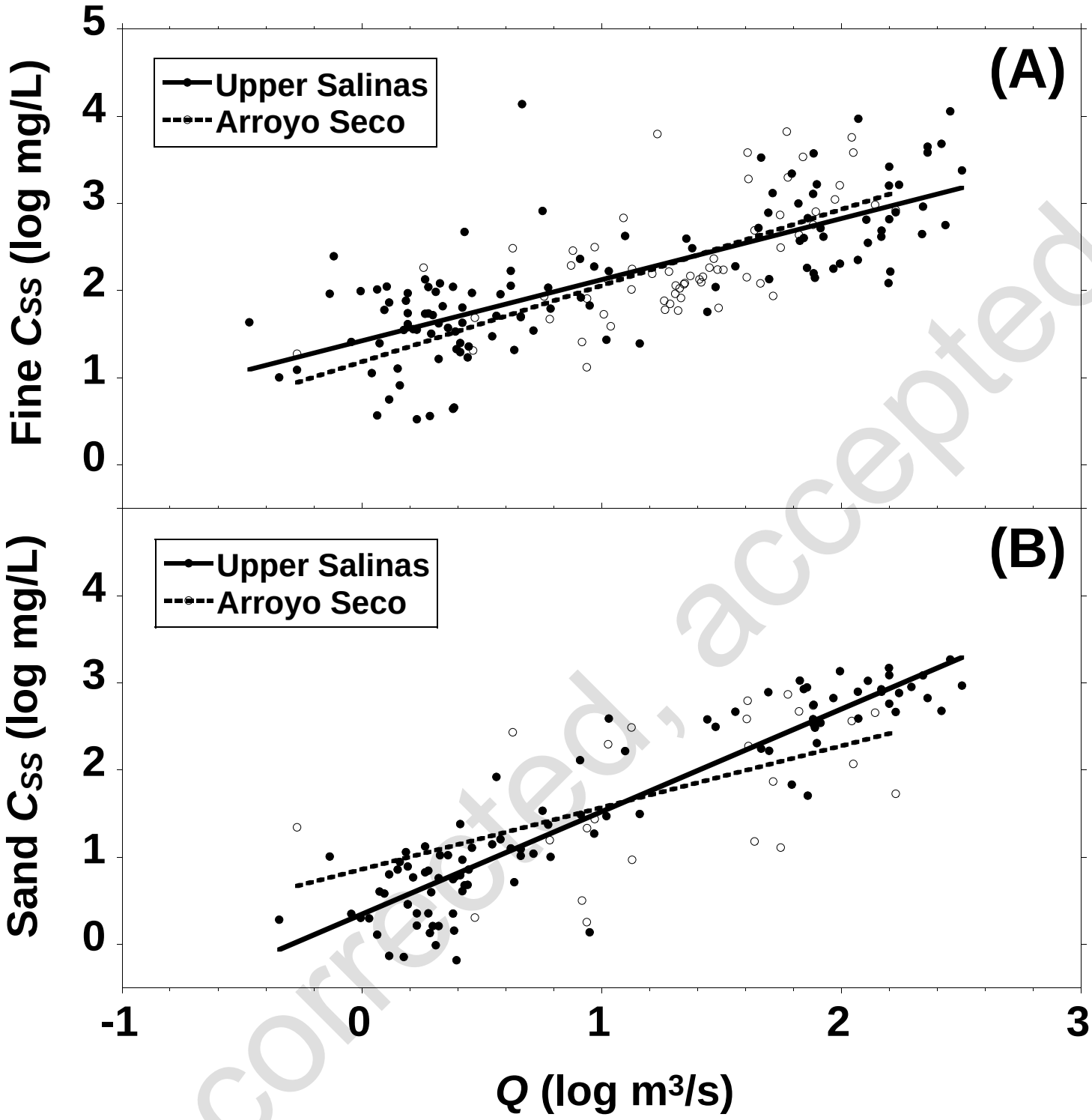

Figure 10.

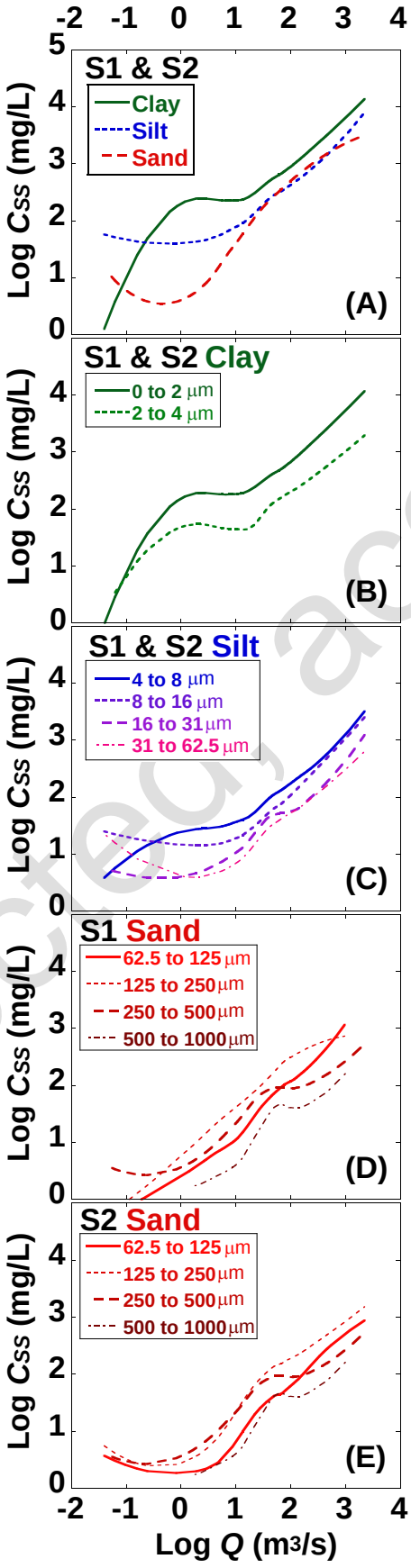

Figure 11.

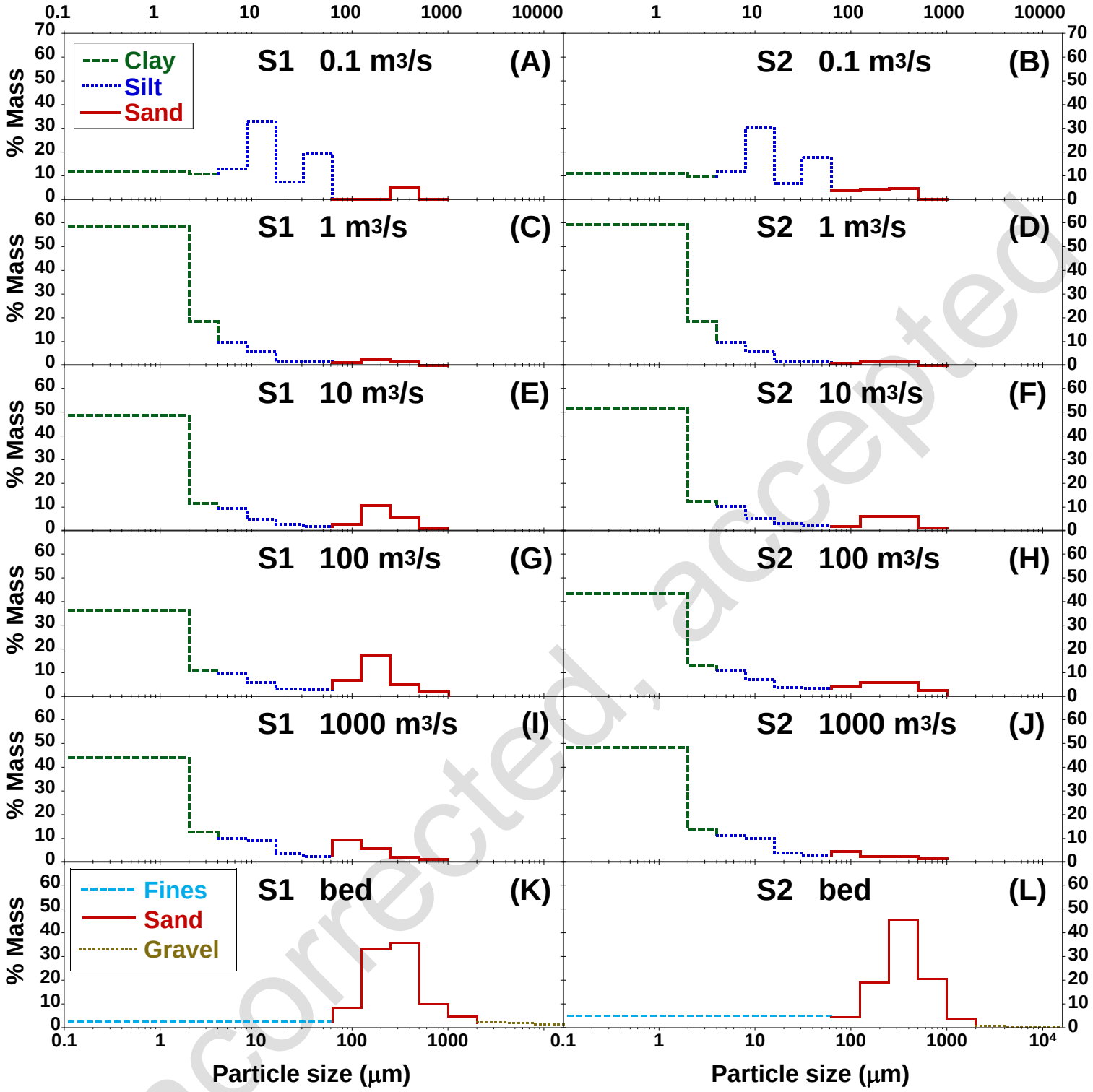

Figure 12.

Supplemental Material I: Bias Testing

Merging suspended sediment samples from two studies extended the temporal range of analysis, but both sample sets (USGS and those collected for this study) included samples from two locations (S1 and S2), and the proportional contribution of these two sites to the total data set was not stable over time (Fig. 2). Selecting only USGS samples with particle size data could also bias analyses because of potential differences between samples with and without particle size data (Table SI.1).

Bias concerns were first addressed by constructing C_{SS}-Q rating curves (see section 4) for subgroups defined by sampling site (S1 or S2), or whether USGS particle size distribution analysis was performed. These subgroup rating curves were then tested for significant differences in the C_{SS}-Q relationship using ANCOVA methods (see section 6.1 and Supplemental Material II). The rating curves subgroups for the particle size distribution categories utilized total C_{SS} data ($C_{SSf} + C_{SSs}$); all others were based on C_{SSf}. Assessment of differences between S1 and S2 suspended sediment behavior was based on data from water years when samples were collected from both sites, and was further broken down into two time periods: {1969,78,79,86} and 2008-2011 to avoid confounding with potential temporal trends. The particle size distribution subgroup comparisons were also performed on data from subsets defined by decade. In order to investigate the effect of omitting USGS samples without particle size data from this study, the rating curve for the entire USGS dataset was compared to the subgroup of samples with associated particle size data.

All bias investigations through rating curve comparisons produced no statistically

significant differences for the entire period of record, except for one incidence of non-coincidence between samples with and without particle size data. The rating curves in this case were found to have offsets and slopes that were not significantly different, and the comparison of rating curves with particle size data to the entire USGS sample set showed that the rating curve was not significantly changed by the inclusion of samples without particle size data. Furthermore, only 30 of 317 suspended sediment samples collected by the USGS were not processed for particle size distribution analysis (see Table SI.1). Thus, selection of the suspended sediment sample set for those that have associated particle size data, and inclusion of samples from stations S1 and S2 were found to have no significant biasing effect on the analyses of suspended sediment behavior in the lower Salinas River.

Supplemental Material II: The ANCOVA Method of Rating Curve Comparison

For ANCOVA comparison between suspended sediment subgroups, multiple regression models were constructed from data subsets using the following general model for two group comparison as per Larsen (2003):

$$\mathrm{Log}(C_{SS}) = \beta_0 + \beta_1 \mathrm{Log}(Q_i) + \beta_2 Z + \beta_3 (\mathrm{Log} Q_i) Z + \varepsilon \qquad \text{(SII.1)}$$

where *Z* is a synthetic variable categorizing the data into any two subsets using a value of 1 or 0, β values are regression fitted coefficients and ε represents random variation not accounted for by the rest of the model. The model for the relationships between

Log(Q) and Log(C_{SS}) for the two groups can then be defined as:

G1 (Z = 1): $$\mathrm{Log}(C_{SS}) = (\beta_0 + \beta_2) + (\beta_1 + \beta_3)\mathrm{Log}(Qi) + \varepsilon \quad \text{(SII.2)}$$

G2 (Z = 0): $$\mathrm{Log}(C_{SS}) = \beta_0 + \beta_1 \mathrm{Log}(Q_i) + \varepsilon \quad \text{(SII.3)}$$

These models form the basis for testing the subgroup rating curves for coincidence, where both subgroups should be described by the same rating curve, parallelism, the condition where rating curve slopes are statistically the same, and offset equivalence, where rating curve intercepts are equal. Coincident subgroups display the exact same relationship between the dependent and independent variables, in this case log(C_{SS}) and log(Q). In testing for coincidence the null hypothesis is:

H_0: $$\beta_2 = \beta_3 = 0. \quad \text{(SII.4)}$$

If the null hypothesis cannot be discarded, then both groups are considered coincident, and the relationship between log(C_{SS}) and log(Q) is described as Eq. 3 for the entire data set. If the null hypothesis is discarded, then further tests for parallelism and equivalence of offset (also known as equality of intercepts or elevation equivalence) are required to determine how the relationship between log(C_{SS}) and log(Q) significantly differ. The null hypothesis of parallelism, the condition in which the slopes of the two subgroup regression lines are equal, is:

H_0: $\beta_3 = 0.$ (SII.5)

Similarly, difference in offset requires only that the intercepts of the two subsets are significantly different, with a null hypothesis of:

H_0: $\beta_2 = 0.$ (SII.6)